NEW SUPPORTED METAL PHOTOCATALYSTS FOR SYNTHESIS OF FINE ORGANIC CHEMICALS DRIVEN BY VISIBLE LIGHT

Zhe Liu

Bachelor of Science (Chemistry)

Thesis completed under supervision of Prof. Huaiyong Zhu, submitted to Queensland University of Technology, in fulfilment of the requirements for the degree of Master of Applied Science

School of Chemistry, Physics and Mechanical Engineering

Science and Engineering Faculty

Queensland University of Technology

2016

Keywords

Abstract

Photocatalysis attracts increasing attention in modern society, because it can drive chemical reactions using solar energy, a reliable, green and abundant energy source. Titanium dioxide (TiO_2) has been widely used as photocatalyst, however it can only absorb UV light that accounts for only 4% of the total solar energy; whereas visible light account for a large fraction (approximately 43%). Thus, for photocatalysis a challenging is utilsing visible light. Recently, nanoparticles (NPs) of plasmonic metals such as gold, silver and copper emerged as a class of new photocatalysts which can strongly absorb visible light. This project aims at developing new plasmonic metal-based photocatalysts that can exhibit high activity for organic reactions under visible light irradiation at moderate conditions.

Firstly, we focused on a more economic plasmonic metal − silver (Ag), because Ag NPs exhibit strong absorption in the range of visible light spectrum, showing possibility to utilize visible light. Therefore Ag NPs supported on zirconium dioxide (ZrO_2) was prepared, and the catalysts thus obtained can selectively catalyze reduction of nitroarenes to azo compounds in visible irradiation at ambient conditions. Furthermore, it was found that supported Ag NPs photocatalyst was also efficient in selective oxidation reactions. The photocatalyst exhibited excellent catalytic activity for selective oxidation of aromatic alcohols under visible light. The catalytic activities of the supported Ag NPs in both reduction and oxidation were sensitive to the intensities and the wavelength of incident light, as well as the reaction temperature. Moreover, supported Ag NPs are recyclable heterogeneous photocatalyst, the NPs are stable in metallic state and showed good reusability.

To extend the application of supported Ag NP photocatalyst, we designed to incorporate copper (Cu) into Ag NPs to obtain Ag-Cu alloy NPs, because Cu exhibits

catalytic activity for many chemical reactions but Cu NPs is to be oxidized in air, which is a limit to the application of pure Cu NPs, although it exhibits strong absorption in visible range. To stablize metallic Cu, we tried Ag-Cu alloy NPs of different Ag:Cu ratios; and found that the alloy NPs with Ag:Cu molar ratio of 4-1 showed the best performance. When Ag-Cu alloy NPs was used as photocatalyst in reduction of nitroarenes, the product is azoxy compounds rather than azo compounds obtained by using the photocatalyst of pure Ag NPs under identical conditions. This is an interesting phenomenon reveals the possibility of alloying another metal into photocatalyst to control the product selectivity. As a result, we plan to apply the alloy NPs in more chemical reactions and compare the mechanism with those using pure Ag NPs and Cu NPs as photocatalyst. We also found that the influence of the NPs size and shape on light absorption and reaction rate is another significant part of our future research.

Overall, the discovery of these new metal NP photocatalysts for organic synthesis reveals new photocatalytic mechanisms for the controlled transformation of chemical synthesis driven by visible light. The results of this project may inspire further studies on other efficient photocatalyst and enhance the potential to utilize sunlight via a controlled and environmental friendly process.

List of Publications

Journal Publications

1. **<u>Zhe Liu</u>**, Yiming Huang, Qi Xiao* and Huaiyong Zhu, Selective Reduction of Nitroaromatics to Azoxy Compounds on Supported Ag-Cu Alloy Nanoparticles through Visible Light Irradiation, *Green Chemistry*, **2015,** doi: 10.1039/c5gc01726b (IF=8.02).

2. Qi Xiao, **<u>Zhe Liu</u>**, Arixin Bo, Sifani Zavahir, Sarina Sarina, Steven Bottle, James D. Riches, and Huaiyong Zhu*, Catalytic transformation of aliphatic alcohols to corresponding esters in O_2 under neutral conditions using visible-light irradiation, *Journal of the American Chemical Society*, **2015**, *137*, 1956-1966 (IF=12.113).

Manuscript submitted

1. **<u>Zhe Liu</u>**, Yiming Huang, Qi Xiao and Huaiyong Zhu*, Application of Supported Silver Nanoparticles as Photocatalyst in Visible Light Irradiation.

2. Qi Xiao, **<u>Zhe Liu</u>** and Huaiyong Zhu*, Tuning the Reduction Power of Visible-Light Photocatalysts of Gold Nanoparticles for Selective Reduction of Nitroaromatics to Azoxy-compounds—Tailoring the Catalyst Support.

3. F. Sifani Zavahir, Kristy Vernon, Sarina Sarina, **<u>Zhe Liu</u>** and Huai-Yong Zhu*. Mesoporous Silica Supported Gold Catalyst for Redox Reactions under Visible Light Irradiation and Its Correlation with Field Enhancement.

List of Abbreviations

Au   Gold

Ag   Silver

Cu   Copper

NP   Nanoparticle

LSPR   Localized Surface Plasmon Resonance

SEM   Scanning Electron Microscopy

TEM   Transmission Electron Microscopy

UV   Ultraviolet

UV-Vis   Ultraviolet Visible

XPS   X-ray Photoelectron Spectroscopy

XRD   X-ray Diffraction

EDX   Energy Dispersive X-ray Spectroscopy

TON   Turnover Number

TOF   Turnover Frequency

Statement of Original Authorship

The work contained in this thesis has not been previously submitted to meet requirement for an award at this or any other higher education institution. To the best of my knowledge and belief, the thesis contains no material previously published or written by another person except where due reference is made.

QUT Verified Signature

Signature:

Date: 17 /05 /2016

Acknowledgements

I would like to deliver my thanks to all those who have helped and supported me throughout the two-year study.

Firstly, I would like to express my sincere gratitude and appreciation to my research supervisor Prof. Huaiyong Zhu, for giving me guidance, inspiration, caring, valuable scientific knowledge and research experiences.

Great acknowledgements are to my senior colleague Dr. Qi Xiao, for the valuable suggestions and patience on my research.

My sincere appreciations also extend to Dr. Chris Carvalho, Leonora Newby and other technicians who have provided assistance at instruments technology. Many thanks to Mr. Tony Raftery for his teaching and assistance with XRD.

Special thanks, of course, go to my dear colleagues: Yiming Huang, Gallage Sunari Peiris, Arixin Bo, Fan Wang and Pengfei Han, who lent me a helping hand in conducting the lab work.

Table of Contents

Chapter 1:

Introduction and Literature Review

1.1 Introduction

With the development of the society and industry, energy consumption is steadily increasing. We now rely mainly on non-renewable sources such as fossil fuels. It is publicly known that solar energy accounts is about 10,000 times a year more than the current global energy consumption.[1] In other words, if we could only exploit 0.01% of solar energy, we would be able to solve the problem of energy shortage. In this context, "green chemical industry" attracts significant attention, especially in the commercial manufacture.[2,3] The outcome of driving synthetic reactions under milder conditions instead of high temperature and pressure will make a great contribution to the industry. Furthermore, the use of solar energy instead of fossil fuels not only alleviates energy shortage but also contributes to our environment. Numerous fine organic chemicals are synthesized via thermal reactions to enhance conversion and get better reaction efficiency. However these often require high temperatures making them energy intensive. A disadvantage of the thermal reactions at high temperature is the poor product selectivity that substantial amount of by-products are generated. If we can drive the organic synthesis at moderate conditions via sunlight or focused sunlight, the dependable, ample and green energy source that produces negligible pollution, this would be an immense achievement. As a result, photocatalysis is a quickly developing area of energy conversion research, because it represents a new way to transfer solar energy into chemical energy.

1.2 Literature Review

1.2.1 Semiconductor Photocatalyst

The research of photocatalysis started since 1960s.[4,5] In 1972 when Honda-Fujishima[8] reported that on TiO_2 electrodes solar energy can be exploited for the generation of hydrogen by water splitting, which was a milestone event. Since then, great efforts have been made on TiO_2-based semiconductor photocatalysts, our group also contributed to this subject.[9,10] The research on TiO_2 semiconductor photocatalysis has been focused on understandingthe mechanism,[6] improving the efficiency of photocatalyst, and expanding the scope of applications.[7] As one of the most popular photocatalysts, TiO_2 not only shows the high activity in several reactions, but also plays a significant role in the application in environmental remediation.[11]

However, the application of the semiconductor photocatalysts is impeded due to several drawbacks. First of all, wide band gap (3.0 - 3.2 eV) allows only UV light absorption by TiO_2 itself. Secondly, the high chance of the electron (e^-)-hole (h^+) recombination decreased the quantum efficiency, which requires co-catalyst loading to prevent the recombination.[12] The charge density on the TiO_2 surface is relatively low. (Figure 1)
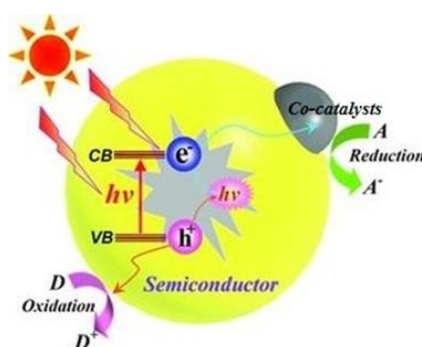

Figure 1. Mechanism of semiconductor photocatalysis process.[12]

In organic synthesis, the product selectivity is of great importance, especially in the production of fine chemicals. However, the use of TiO_2-based photocatalysts has a potential

problem that most organic compounds often undergo uncontrolled oxidation. Although several synthetic reactions have been proved to proceed in TiO_2-modified heterogeneous photocatalytic systems, conversion is relatively low and it seems that high selectivity is only limited to a few appropriate substrates.[13]

Another problem with conventional semiconductor photocatalysts is that they can only absorb UV light (wavelength < 400 nm) which accounts only a small fraction of solar spectrum. As a result, effective utilization of full solar spectrum where the visible light accounts for more than 40% of the solar energy, has been long 'dream' of the photocatalysis researchers.[14] Thus, it is important to search new photocatalysts that are capable of inducing the reactions with high selectivity under visible light irradiation, which will be a promising target of industrial synthesis.

1.2.2 Noble Metal Photocatalysts

It has been found that plasmonic metal NPs exhibit excellent catalytic activity in organic synthesis because they can strongly absorb visible light.[15-18] A key feature of plasmonic metal nanostructures is their strong interaction with resonant incident photons through excitation of the localized surface plasmon resonance (LSPR). The LSPR is the photon-induced collective oscillation of conduction electrons, established when the frequency of the incident light is resonant with the natural oscillation frequency of metal's free electrons in response to the restoring force of the positive nuclei (Figure 2). The oscillation of electrons may create an intense electromagnetic field concentrated near the metal nanostructure's surface (<100 nm).[17] This intense localized field associated with the plasmonic metal nanostructures leads to their application in various fields, such as solar cells,[16] surface-enhanced Raman spectroscopy,[19,20] molecular sensing in biological systems,[21] single-molecule spectroscopy,[20, 22, 23] and many others.[24] It is also known that the particle size and shape of metal

nanostructures have a significant influence on the optical properties of plasmonic metals, therefore the study on the geometry of the structures is a promising direction in the area of metal NP photocatalysts.[25, 26]
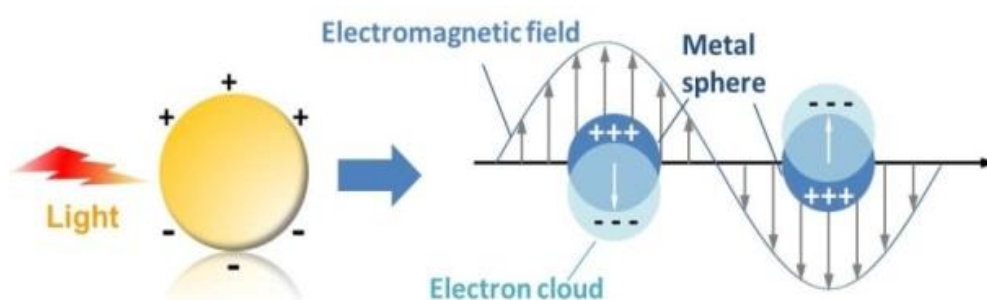

Figure 2. Localized surface plasmons resonance (LSPR) effect of a metal nanosphere.[27]

It can be seen that gold (Au), silver (Ag), and copper (Cu) spherical NPs (diameters of particles were approximately 20 nm) showed strong LSPR absorption at 530, 400 and 580 nm respectively (Figure 3) within the visible light range. The resonant interaction of incident light and surface conduction electrons initially leads to the coherent oscillation of electrons that can persist for nearly one picosecond, producing a corresponding intense oscillating electric field near the NP surface that possesses a high concentration of energetic electrons.[28,29] The combination of energized surface electrons, the intense local electric fields, and the well-known catalytic properties of NPs, provides the possibility for plasmonic NPs to be used as direct photocatalysts.[30]
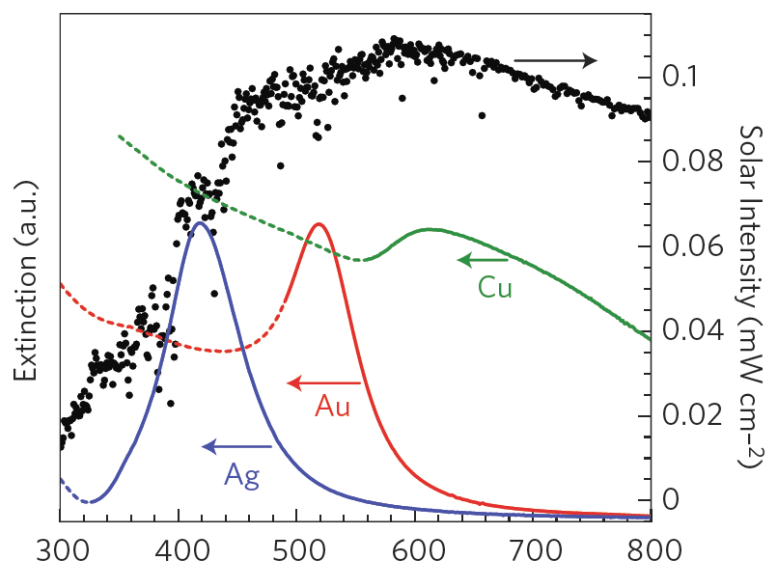
Figure 3. UV-vis absorption spectrum of Au, Ag and Cu NPs.[30]

There are a lot of parameters which can affect the optical properties of plasmonic metal NPs, such as the size and geometry of structure, the values of the dielectric constants of both the surrounding material and the metal.[31] The strength of the enhanced local field can be more than 500 times greater than the applied field when the noble metal nanomaterials have different shapes, like cubes, nanowires, triangular plates and junctions.[32] The research about the influence of nanoparticle shape on LSPR effect has been extensively studied. For silver NPs, an apparent shift of plasmon absorption in the range of visible light spectrum was observed when changing the NP shapes.[17] (Figure 4)
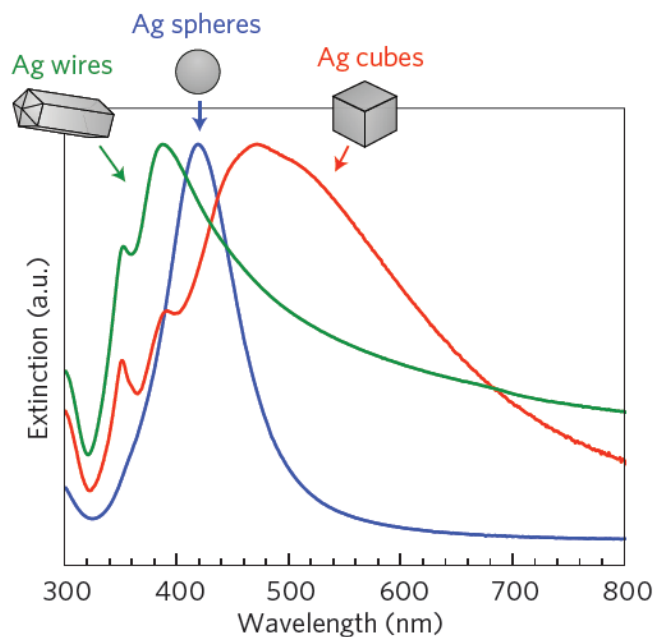
Figure 4. Absorption spectra of silver NPs with different shapes.[17]

In recent years, there have been many reports on the optical properties of gold nanoparticles (Au NPs).[33, 34] If the catalytic activity of gold nanoparticles can be combined to their LSPR absorption, there will be a significant improvement. Zhu et al. verified this assumption by oxidizing some organic compounds under visible light irradiation over gold nanoparticle supported on ZrO_2 and SiO_2.[40] In addition, gold nanoparticles have also been found active in reductive reactions such as nitrobenzene and hydroamination of alkyne.[41] It has been found that Au NPs supported on metal oxides showed excellent catalytic activity for significant chemical oxidations.[35-39] These findings clearly demonstrated that the gold nanoparticle itself has great contribution to photocatalytic activity but not only working as a dopant to narrow the band gap of a semiconductor.

The outstanding properties of noble metal NP photocatalysts include:

(1) Impact of wavelength – tuning the product selectivity

The characteristic of noble metal NPs photocatalysts is that the photocatalytic activity is depend on the incident wavelength, which is different from semiconductor photocatalysts. In

the case of semiconductor photocatalysis, the energy of photons is required to be higher than the band gap of semiconductor to induce the reactions. The wavelength of incident light cannot change the ability of incident light to induce chemical transformation. Metal NPs such as gold can response to all wavelengths of light as following a different mechanism.[42]

To better understand the wavelength impact of Au NP photocatalyzed reductive process, three model reactions were selected in our previous study. The reduction ability of photocatalysts can be tuned by the wavelength of incident light since different reactions have different reduction potentials. It is found that reactant molecules with more negative reduction potentials can only gain energy from the excited electrons of Au NPs when these electrons occupy higher energy levers, which can only be excited by the incident light with shorter wavelength. Au NPs exhibit weak light absorption if the wavelength is longer than 650 nm, so the conversion of these reactions is low. (Figure 5)
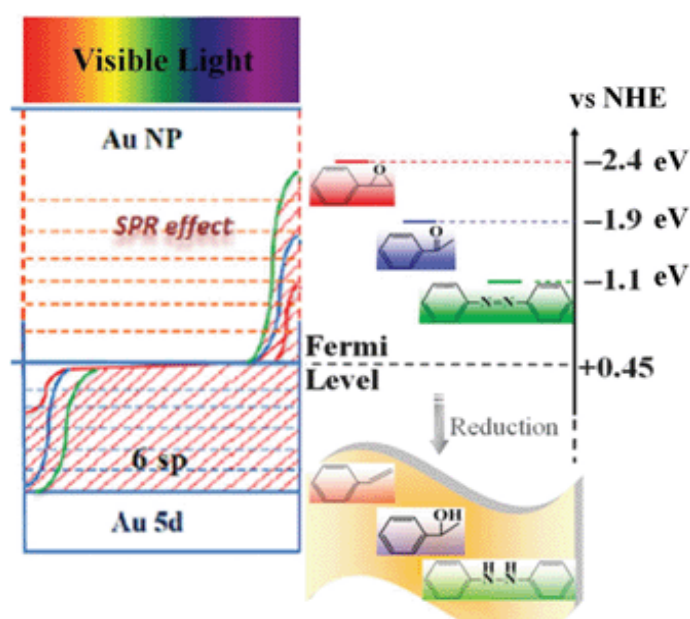

Figure 5. Schematic of reduction reactions catalyzed by supported Au NPs in different ranges of wavelength [42]

(2) Impact of light intensity

The positive relationship of photocatalytic activity with light intensities is also a typical feature of metal NPs photocatalysts. For example, the oxidation of HCHO catalyzed by Au@ZrO$_2$ was influenced by the intensity of incident light. It can be seen from Figure 6 that no changes were detected if the reaction was conducted in dark. However in the photocatalytic reactions, the conversion increases with the raising of irradiance light intensity. As result, it can be confirmed that this reaction was driven by visible light.
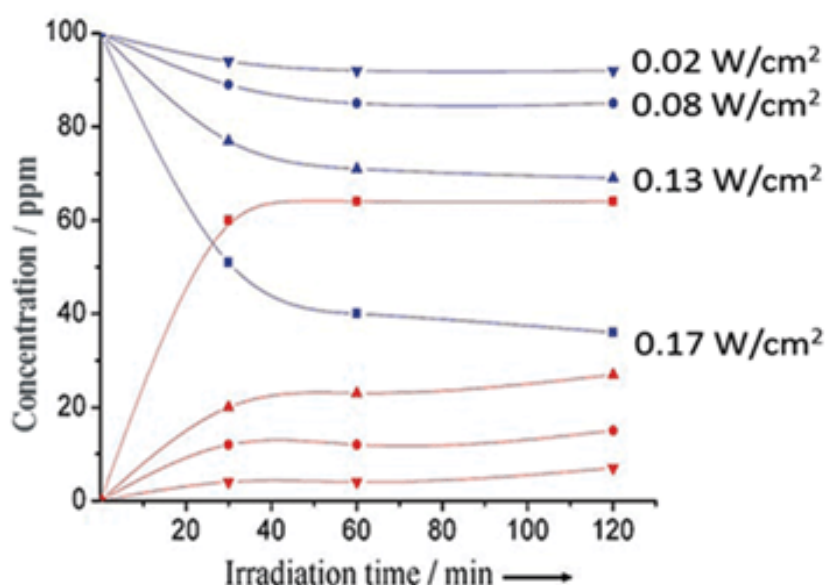

Figure 6. Oxidation of HCHO catalyzed by Au@ZrO$_2$ with the irradiation of blue light [43]

1.2.3 Alloy Nanoparticle Photocatalysts

It should be noted that the number of chemical reactions which can be catalyzed by Au NPs is limited compared with that with those non-plasmonic transition metals. It is well known that catalytically active palladium (Pd) is widely used in organic synthesis. As a result, our group designed the Au-Pd alloy NPs photocatalyst.[44] We found that there are two factors to influence the activity of Au-Pd alloy NPs, one is the light absorption of Au-Pd alloy NPs, and another is the catalytically active Pd site on the surface of the NPs. The molar ratio of Au-Pd alloy NPs is a key factor for the preparation of alloy NPs. Furthermore, the activity of the

alloy NPs catalyst is affected by the wavelength and intensity of incident light. It can be concluded that the absorbed light energy by alloy NPs can generate hot electrons to improve the catalytic activity of Pd. [44, 45]

1.2.4 The Photocatalytically Inert Supporting Materials

To isolate the individual photocatalytic activity of metal NPs, supporting material shall exhibit no light absorption in the visible range, such as metal oxides with very wide band gaps (ZrO_2, Al_2O_3 and LDH etc.). The support can help to increase the exposure of the catalytic sites of NPs so that the reactant molecules may get more opportunities to engage with the active sites of photocatalyst. Furthermore, the support can avoid the aggregation of NPs efficiently. In addition, reusability is a significant character of heterogeneous catalyst. The supported NPs can be washed with water and ethanol, after that it can be tried for subsequent reactions.

(1) Zirconium dioxide (ZrO_2)

ZrO_2 is a material frequently used in heterogeneous catalysis as support.[46] Owing to its wide band gap, recently it has been considered as an ideal support material for metal nanoparticle photocatalyts. As ZrO_2 does not absorb visible light by itself and it is easier to identify the contribution from LSPR absorption by the supported metal NPs.[47, 48] Consequently, the catalytic activity could not be simply explained by the same mechanism as occurs in those typical semiconductor photocatalysts, but mainly due to the LSPR effect of metal nanoparticles under visible irradiation.[33]

(2) Layered double hydroxides (LDH)

Layered double hydroxides (LDH) are anionic clay matrices that consist of bruited ($Mg(OH)_2$)-like positively charged two-dimensional sheets in which some divalent cations such as Mg^{2+} are substituted by trivalent cations, further, water and exchangeable charge-compensating anions are present in the interlayer.[49] Infinite two dimensional sheets consist of

several edge-sharing MgO_6 octahedral units in which divalent and trivalent cations are six-fold coordinated to OH^-. The positive charge on the sheets is compensated by anions such as CO_3^{2-} intercalated in the interlayers. LDH has been used as support in catalysts, however the application in photocatalysis process is rarely reported. It has been demonstrated that LDH is a promising support material for Au NP in the catalytic oxidation,[50] dehydrogenation,[51] and deoxygenation[52] of organic chemicals. Furthermore, LDH solids are known to possess surface basic properties that can be fine-tuned by their compositions. Our group has found that the phosphate modified LDH support ($LDH-PO_4^{3-}$) can be prepared by ion exchange to introduce phosphate anions utilizing the "memory effect". As a result, for the esterification of aliphatic alcohol, basic sites are present as part of the supporting material, the addition of base was not required.[53]

1.2.5 Application of Metal Nanoparticles as Photocatalyst

The optical property of LSPR absorption gives the noble metal a potential capability of driving chemical reactions in an efficient way by utilizing the visible light, which will enable us to use the full spectrum of solar energy.

1.2.5.1 Reactions catalyzed by Au NPs

Au NPs exhibits excellent photoactivity because of LSPR light absorption, which was first found in the degradation of volatile organic compound in visible light irradiation at mild conditions.[43] After that, many applications of Au NPs as photocatalyst was found in addition to the degradation of chemical pollutants. This provides possibility for the application of solar energy in chemical transformations, which is more environmental friendly than the thermally driven catalysis.

(1) Selective Reductions

Our group has found that Au NPs supported on ZrO_2 ($Au@ZrO_2$) can be used as photocatalyst in the selective reduction of nitro-aromatic compounds to azo compounds in UV and visible light with high conversion at mild conditions. (Figure 7).[38]
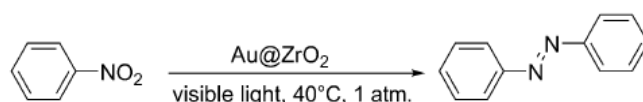

Figure 7. Reduction of nitro-aromatic compounds to azo compounds with $Au@ZrO_2$ in visible light [38]

It is the first report of azo-benzene synthesis by direct reductive coupling of nitroaromatic compounds in moderate conditions, which is different from the condition of thermally catalyzed reaction. The reaction can be catalyzed by supported Au NPs under mild conditions, providing opportunity to improve the selectivity to the desired product.

To further analysis the common features of reduction process driven by visible light with Au NPs as photocatalyst, the other three reductions were conducted in mild surrounding environment: deoxygenation of epoxides to alkenes, reduction of ketones to alcohols, and hydrogenation of azobenzene to hydroazobenzene.[42] (Figure 8)
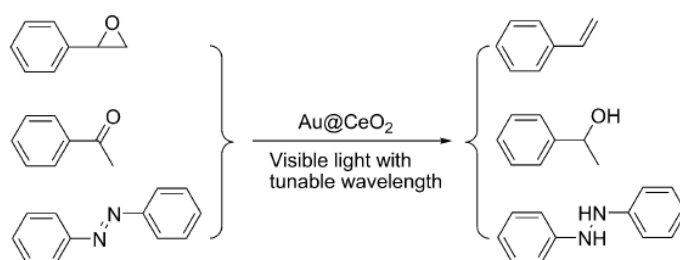

Figure 8. Photocatalytic reductive reactions with Au NPs in light irradiation [42]

(2) Selective Oxidations

In addition to reduction reactions, Au NPs shows excellent photocatalytic activity in many oxidation reactions. It has been reported by Zheng et al. that the noble metal photocatalysts

supported on TiO_2 showed excellent activity in the oxidation of benzene, in which Au performed best.[54] It was found by Tanaka et al. that $Au@CeO_2$ could catalyze the oxidation of benzyl alcohol in the irradiation of green LED light with wavelength of 530 nm.[55] The positive relationship between surface area of Au NPs supported on CeO_2 and the reaction conversion can be observed. It shows that the factor which influences on the activity of photocatalyst is not the amount of Au loaded on CeO_2, but the external surface area of Au NPs. (Figure 9)
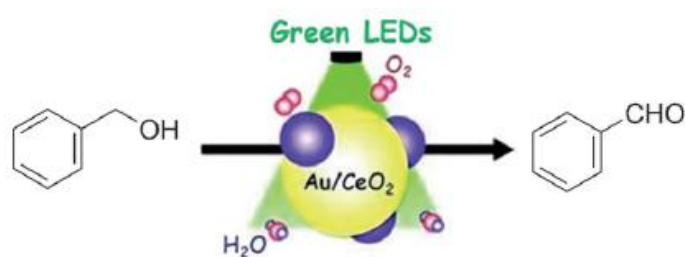
Figure 9. Selective oxidation of benzyl alcohol with $Au@CeO_2$ in green light irradiation with wavelength of 530 nm [55]

It has been reported by Zhang et al. that Au NPs supported on zeolite Y showed excellent activity in the oxidation of aromatic alcohols to aldehydes under visible light irradiation under mild conditions.[56] The zeolite supports could concentrate reactants at room temperature and the conversions of aromatic alcohols depended on their molecular polarities. It can be found from the experiment results that the activity of Au@zeolite catalyst depended on the adsorptive properties of the zeolite supports, the LSPR light absorption, as well as the particle size and the specific surface areas of the Au NPs. (Figure 10)

Figure 10. Photocatalytic selective oxidation of alcohol with Au@zeolite in light irradiation.[56]

1.2.5.2 Reactions Catalyzed by Ag and Cu NPs

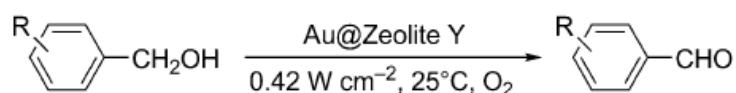We study on the application of Ag NPs supported on photocatalytically inert oxides (such as zeolite Y, ZrO_2 and SiO_2) in oxidation reactions in the irradiation of visible light.[58] It was also reported that $Ag@Al_2O_3$ showed excellent photocatalytic activity in oxidation of ethylene to ethylene oxide, which is an important reaction in industry.[57] Linic's group studied the interaction of O_2 molecules and photo-reduced electrons on the surface of Ag NPs. Furthermore, there has been reported that Ag NPs can be used as high-efficient photocatalyst supported on AgCl and AgBr.[59]

Since the metallic Cu is easily to be oxidized in air, which limits the application of Cu NPs. It has been reported that Cu NPs supported on graphene show excellent photocatalytic activity in reduction of aromatic nitro compounds to azo and azoxy compounds in visible light with the high conversion and selectivity.[60] The successful application of Cu NPs inspires the study of supporting materials which can protect the metal NPs from oxidation, this can expand the application of Cu NPs as photocatalyst for many reactions. (Figure 11)

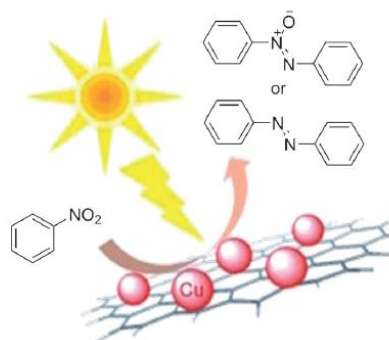Figure 11. Reduction of aromatic nitro compounds with Cu@graphene in visible light [59]

1.2.5.3 Reactions Catalyzed by Alloy NPs

It is obvious that there is a limitation for plasmonic metals to catalyze different kinds of chemical reactions, while many non-plasmonic transition metals exhibit excellent catalytic activity to some important reactions. As a result, they are widely used as catalyst for chemical

transformation but they are seldom used as photocatalysts. Palladium (Pd) is well-known to show catalytic activity for lots of important chemical reactions because it has strong affinity to many orgainc molecules. It has been reported by our group that the Au-Pd alloy NPs can be utilized in many reactions.[44] Furthermore; our group has found that the combination of Au-Pd alloy NPs and LDH-PO$_4^{3-}$ can catalyze the esterification of aliphatic alcohols in mild condition using visible light irradiation, which is a great improvement in application of alloy photocatalysis.[53]

1.3 Summary

This chapter briefly reviews the development of photocatalysts, from semiconductor to metal nanoparticle photocatlysts. The direct plasmonic photocatalysts performed well in enhancing the reaction rate under mild conditions, which is achieved with thermally catalyzed reactions. Furthermore, it should be an important area to research the influence factor on the LSPR light absorption, including the particle size and shape, which provides us the possibility to improve the reaction rate and the selectivity by designing metal nanostructures. Moreover, the use of gold and silver NPs is limited; the use of copper can be conducted to expand the application scope of plasmonic metals.

In summary, study on the NPs of metals to improve the reaction rate by light irradiation is of great significance. Utilizing LSPR effect of metal NPs in photocatalysis is of great significant, which provides the possibility to utilize solar energy efficiently, at the same time there is more improvement for our researchers to achieve.

Reference list

1. M. Gratzel, *Nature*, 2001, **414**, 338-344.

2. M. Poliakoff and P. Licence, *Nature*, 2007, **450**, 810-812.

3. V. Gewin, *Nature*, 2006, **440**, 378-379.

4. H. D. Muller and F. Steinbach, *Nature*, 1970, **225**, 728-729.

5. F. Steinbach, *Nature*, 1969, **221**, 657-658.

6. M. R. Hoffmann, S. T. Martin, W. Choi and D. W. Bahnemann, *Chem. Rev.*, 1995, **95**, 69-96.

7. Mills and S. Le Hunte, *J. Photochem. Photobiol. A, Chem.*, 1997, **108**, 1-35.

8. K. Sunada, Y. Kikuchi, K. Hashimoto and A. Fujishima, *Environ. Sci. Technol.*, 1998, **32**, 726-728.

9. Z. Zheng, J. Zhao, Y. Yuan, H. Liu, D. Yang, S. Sarina, H. Zhang, E. R. Waclawika and H. Zhu, *Chem.–Eur. J.*, 2013, **19**, 5731-5741.

10. D. Yang, C. Chen, Z. Zheng, H. Liu, E. R. Waclawik, Z. Yan, Y. Huang, H. Zhang, J. Zhao and H. Zhu, *Energy. Environ. Sci.*, 2011, **4**, 2279-2287.

11. S. C. Roy, O. K. Varghese, M. Paulose and C. A. Grimes, *ACS. Nano.*, 2010, **4**, 1259-1278.

12. H. Tong, S. Ouyang, Y. Bi, N. Umezawa, M. Oshikiri and J. Ye, *Adv. Mater.*, 2012, **24**, 229-251.

13. Y. Shiraishi and T. Hirai, *J. Photoch. Photobio. C*, 2008, **9**, 157-170.

14. J. Zhao, C. Chen and W. Ma, *Top. Catal.*, 2005, **35**, 269-278.

15. P. V. Kamat, *The J. Phys. Chem. B*, 2002, **106**, 7729-7744.

16. L. Qiao, D. Wang, L. Zuo, Y. Ye, J. Qian, H. Chen and S. He, *Appl. Energy.*, 2011, **88**, 848-852.

17. S. Linic, P. Christopher and D. B. Ingram, *Nat Mater*, 2011, **10**, 911-921.

18. K. Watanabe, D. Menzel, N. Nilius and H.-J. Freund, *Chem. Rev.*, 2006, **106**, 4301-4320.

19. M. Potara, A.-M. Gabudean and S. Astilean, *J. Mater. Chem.*, 2011, **21**, 3625-3633.

20. S. Nie and S. R. Emory, *Science*, 1997, **275**, 1102-1106.

21. J. N. Anker, W. P. Hall, O. Lyandres, N. C. Shah, J. Zhao and R. P. Van Duyne, *Nat Mater*, 2008, **7**, 442-453.

22. S. Kühn, U. Håkanson, L. Rogobete and V. Sandoghdar, *Phys. Rev. Lett.*, 2006, **97**, 017402.

23. Jiang, K. Bosnick, M. Maillard and L. Brus, *J. Phys. Chem. B*, 2003, **107**, 9964-9972.

24. E. M. Larsson, C. Langhammer, I. Zorić and B. Kasemo, *Science*, 2009, **326**, 1091-1094.

25. M. Rycenga, C. M. Cobley, J. Zeng, W. Li, C. H. Moran, Q. Zhang, D. Qin and Y. Xia, *Chem. Rev.*, 2011, **111**, 3669-3712.

26. Y. Xia, Y. Xiong, B. Lim and S. E. Skrabalak, *Angew. Chem. Int. Ed.*, 2009, **48**, 60-103.

27. X. Lu, M. Rycenga, S. E. Skrabalak, B. Wiley and Y. Xia, *Annu. Rev. Phys. Chem.*, 2009, **60**, 167-192.

28. S. Link and M. A. El-Sayed, *Int. Rev. Phys. Chem.*, 2000, **19**, 409-453.

29. L. Brus, *Acc. Chem. Res.*, 2008, **41**, 1742-1749.

30. S. Linic, P. Christopher, H. Xin and A. Marimuthu, *Acc. Chem. Res.*, 2013, **46**, 1890-1899.

31. L. M. Liz-Marzán, *Langmuir*, 2006, **22**, 32-41.

32. S. Eustis and M. A. El-Sayed, *Chem. Soc. Rev.*, 2006, **35**, 209-217.

33. X. Huang, I. H. El-Sayed, W. Qian and M. A. El-Sayed, *J. Am. Chem. Soc.*, 2006, **128**, 2115-2120.

34. M. Haruta, *Gold. Bull.*, 2004, **37**, 27-36.

35. M. D. Hughes, Y.-J. Xu, P. Jenkins, P. McMorn, P. Landon, D. I. Enache, A. F. Carley, G. A. Attard, G. J. Hutchings, F. King, E. H. Stitt, P. Johnston, K. Griffin and C. J. Kiely, *Nature*, 2005, **437**, 1132-1135.

36. M. Valden, X. Lai and D. W. Goodman, *Science*, 1998, **281**, 1647-1650.

37. Q. Fu, H. Saltsburg and M. Flytzani-Stephanopoulos, *Science*, 2003, **301**, 935-938.

38. H. Zhu, X. Ke, X. Yang, S. Sarina and H. Liu, *Angew. Chem. Int. Ed.*, 2010, **122**, 9851-9855.

39. S. Sarina, E. R. Waclawik and H. Zhu, *Green. Chem.*, 2013, **15**, 1814-1833.

40. X. Chen, H.-Y. Zhu, J.-C. Zhao, Z.-F. Zheng and X.-P. Gao, *Angew. Chem. Int. Ed.*, 2008, **120**, 5433-5436.

41. J. Zhao, Z. Zheng, S. Bottle, A. Chou, S. Sarina and H. Zhu, *Chem. Commun.*, 2013, **49**, 2676-2678.

42. X. Ke, S. Sarina, J. Zhao, X. Zhang, J. Chang and H. Zhu, *Chem. Commun.*, 2012, **48**, 3509-3511.

43. X. Chen, H. Y. Zhu, J. C. Zhao, Z. F. Zheng and X. P. Gao, *Angew. Chem. Int. Ed.*, 2008, **120**, 5433-5436.

44. S. Sarina, H. Zhu, E. Jaatinen, Q. Xiao, H. Liu, J. Jia, C. Chen and J. Zhao, *J. Am. Chem. Soc.*, 2013, **135**, 5793-5801.

45. Q. Xiao, S. Sarina, A. Bo, J. Jia, H. Liu, D. P. Arnold, Y. Huang, H. Wu and H. Zhu, *ACS. Catal.*, 2014, **4**, 1725-1734.

46. Navío, Hidalgo, G. Colón, S. G. Botta and M. I. Litter, *Langmuir*, 2000, **17**, 202-210.

47. S. Sarina, H.-Y. Zhu, Q. Xiao, E. Jaatinen, J. Jia, Y. Huang, Z. Zheng and H. Wu, *Angew. Chem. Int. Ed.*, 2014, **126**, 2979-2984.

48. N. Lopez and J. K. Nørskov, *J. Am. Chem. Soc.*, 2002, **124**, 11262-11263.

49. G. Fornasari, M. Gazzano, D. Matteuzzi, F. Trifirò and A. Vaccari, *Appl. Clay. Sci.*, 1995, **10**, 69-82.

50. T. Mitsudome, A. Noujima, T. Mizugaki, K. Jitsukawa and K. Kaneda, *Green. Chem.*, 2009, **11**, 793-797.

51. W. Fang, Q. Zhang, J. Chen, W. Deng and Y. Wang, *Chem. Commun.*, 2010, **46**, 1547-1549.

52. Noujima, T. Mitsudome, T. Mizugaki, K. Jitsukawa and K. Kaneda, *Angew. Chem. Int. Ed.*, 2011, **50**, 2986-2989.

53. Q. Xiao, Z. Liu, A. Bo, S. Zavahir, S. Sarina, S. Bottle, J. D. Riches and H. Zhu, *J. Am. Chem. Soc*., 2015, **137**, 1956-1966.

54. Z. Zheng, B. Huang, X. Qin, X. Zhang, Y. Dai and M.-H. Whangbo, *J. Mater. Chem.*, 2011, **21**, 9079-9087.

55. A. Tanaka, K. Hashimoto and H. Kominami, *Chem. Commun.*, 2011, **47**, 10446-10448.

56. X. Zhang, X. Ke and H. Zhu, *Chem. Eur. J.*, 2012, **18**, 8048-8056.

57. P. Christopher, H. Xin and S. Linic, *Nat.Chem.*, 2011, **3**, 467-472.

58. X. Chen, Z. Zheng, X. Ke, E. Jaatinen, T. Xie, D. Wang, C. Guo, J. Zhao and H. Zhu, *Green. Chem.*, 2010, **12**, 414-419.

59. H. Chen, L. Shao, Q. Li and J. Wang, *Chem. Soc. Rev.*, 2013, **42**, 2679-2724.

60. X. Guo, C. Hao, G. Jin, H. Y. Zhu and X. Y. Guo, *Angew. Chem. Int. Ed.,* 2014, **126**, 2004-2008.

Chapter 2:

Application of Supported Silver Nanoparticles as Photocatalyst in Visible Light Irradiation

Introductory Remarks

In this charter, supported silver nanoparticles (Ag NPs) was designed and synthesized for the redox reactions in the irradiation of visible light in mild conditions. We prepared 3% Ag nanoparticles supported on zirconium dioxide (ZrO_2) as photocatalyst. Ag exhibited strong absorption at about 392 nm wavelength. We found that supported Ag NPs showed sensitive activity in selective reduction of aromatic nitro compound to azo compounds. For example, when the temperature was kept at 60 °C, the conversion in dark was 23% with supported Ag NPs as photocatalyst, while the conversion increased to 87% in the light irradiation at the same temperature. The conversion rate can be enhanced by strengthening light irradiation intensity and increasing the reaction temperature.

Furthermore, this photocatalyst shows good activity in selective oxidation of aromatic alcohol compounds to aromatic aldehyde compounds at mild conditions. The conversion achieved 94% at 60 °C in light irradiation while no product could be tested in dark reaction at the same temperature. To better understand if the reaction occurs via a light-induced process, we conducted the action spectrum to show the relationship between light absorption and reaction rate for both reactions. The research on Ag NP photocatalysts can promote the study on other photocatalysts and improve the application of sunlight to drive chemical reactions.

Statement of Contribution of Co-Authors

Publication title and date of publication or status:

Application of Supported Silver Nanoparticles as Photocatalyst in Visible Light Irradiation

Zhe Liu, Yiming Huang, Qi Xiao and Huaiyong Zhu*

Manuscript submitted

Contributor	Statement of contribution
Student Author: Zhe Liu Signature Date	Discovered the photocatalytic reaction, organized and designed the experiments, conducted the data collection, analyzed the data, proposed the reaction mechanism and wrote the manuscript
Yiming Huang	Analyzed data, offered interpretations, provided the detailed TEM analysis
Qi Xiao	Gave constructive suggestion on the reaction
Prof. Huaiyong Zhu	Proposed the idea and polished the manuscript

Principal Supervisor Confirmation

I have sighted email or other correspondence from all Co-authors confirming their certifying authorship.

QUT Verified Signature

HUAI YONG ZHU   27/10/2015

Name   Signature   Date
                              QUT Verified Signature   1/06/2016

Qi Xiao

Yiming Huang   QUT Verified Signature   1/06/2016.

19

Article:

Supported silver nanoparticles as photocatalysts for organic synthesis reactions through visible irradiation

Zhe Liu, Yiming Huang, Qi Xiao and Huaiyong Zhu*

1. INTRODUCTION

It is of great significant to utilize solar energy to drive chemical reactions in mild conditions, which is a abundant, safe and green energy source.[1,2,3] The plasmon noble mental such as Au, Ag, Cu attracts a lot of attention recently because the nanostructures of the three metals have strong light absorption in the range of visible light.[4] It provides the possibility to utilize visible light to drive chemical reactions in mild conditions.[5] It has been found that supported gold (Au) nanoparticles (NPs) can efficiently catalyze couples of reactions via LSPR effect at moderate conditions.[6,7] Very recently it has been found that Cu NPs supported on graphene also exhibit high photocatalytic activity for the reductive coupling of nitroaromatics to aromatic azo-compounds under irradiation of solar spectrum.[5] In addition to Cu NPs, Ag NPs exists excellent photocatalytic activity in organic synthesis.[8] It has been reported that supported Ag NPs on semiconductor (TiO_2, CeO_2) can enhance the catalysis for several reactions.[1] In our research, supported Ag NPs on ZrO_2 can directly be used as photocatalyst for redox reactions.

To confirm the wide application of Ag NPs as photocatalyst, two catalytic reactions were conducted, including the reduction of nitroaromatic compounds and the oxidation of benzyl alcohol. The selective reduction of nitroaromatics is important reactions in organic synthesis,[1] which can produce the important industrial intermediates, such as amines, azo and azoxy compounds.[9,10-12] Furthermore, selective oxidation of aromatic alcohols to aldehydes is of

significance in chemical reactions.[13,14] The result investigate that supported Ag NPs perform prominent activity as photocatalyst with visible light.

2. EXPERIMENTAL SECTION

2.1 Catalysts Preparation

3 wt% of silver NPs supported on ZrO_2 ($Ag@ZrO_2$) was prepared by the impregnation−reduction method. For example, Ag NPs was prepared as follow, $AgNO_3$ (94.5 mg) was dissolved into 60mL deionized water, to the above solution ZrO_2 powder (2.0 g) was dispersed followed by adding 10 mL L-lysine aqueous solution (0.01 M). The mixture was kept under magnetic stirring at room temperature for 20 min. To this suspension, 10 mL of freshly prepared aqueous $NaBH_4$ (0.35mol) solution was added dropwise. The mixture was aged for 24h, and then the precipitate was separated by centrifugation, washed with water (three times) and ethanol (once), and dried at 60 °C in vacuum for 24 h. The collected powder was used directly as catalyst.

2.2 Catalysts Characterization

The morphology study of catalysts was carried out on a JEOL 2100 transmission electron microscopy (TEM) equipped with a Gatan Orius SC1000 CCD camera, with an accelerating voltage of 200 kV and nickel grids were used as the supporting film. Diffuse reflectance UV-visible spectra of the sample catalysts were examined by a Varian Cary 5000 spectrometer with $BaSO_4$ as a reference. X-ray diffraction (XRD) patterns of the sample powders were collected using a Philips PANalytical X'pert Pro diffractometer.

2.3 Activity Test

In a typical activity test, a 20 mL Pyrex glass tube was used as the reaction vessel. The vessel containing reactants and catalyst was irradiated with visible light using a halogen lamp (from Nelson, wavelength in the range of 400−750 nm) under magnetic

stirring; the irradiance was measured to be 0.5 W/cm^2. The reaction temperature was carefully controlled with an air conditioner attached to the reaction chamber. The reactions in the dark were conducted using an oil bath placed above a magnetic stirrer to maintain the reaction temperature the same to corresponding reactions with light illuminations; reaction tubes were wrapped with aluminum foil to avoid exposure to light. At given irradiation time intervals, 0.5 mL aliquots were collected, the catalyst particulates was removed by a Millipore filter (pore size 0.45 μm). The liquid−phase products were analyzed by gas chromatography (GC) technique (Agilent 6890) with a HP−5 column to monitor the change in the concentrations of reactants and products. An Agilent HP5973 mass spectrometer was used to identify the product.

Action spectrum experiments: Light emission diode (LED) lamps (Tongyifang, Shenzhen, China) with wave-lengths 360±5 nm, 400±5 nm, 470±5 nm, 530±5 nm, 590±5 nm and 620±5 nm were used as the light source. The environmental temperature was measured to be 60±2 °C, and all the other reaction conditions were identical to those of typical reaction procedures. The AQE was calculated as: AQE = [(Y_{light}−Y_{dark})/(the number of incident photons)]×100%, where Y_{light} and Y_{dark} are the number of products formed under irradiation and dark conditions, respectively.

3. RESULTS AND DISSCUSSION

3.1 Catalyst Synthesis and Characterization

Transmission electron microscopy (TEM) analysis of the Ag NPs shows the catalysts morphology. [15,16] The Ag NPs are well distributed on the ZrO$_2$ crystal surface (Figure 1a). The high resolution (HR)-TEM image indicated that the crystal face of Ag NPs is predominantly (111) face and the space of lattice fringe is 0.23 nm (Figure 2b).
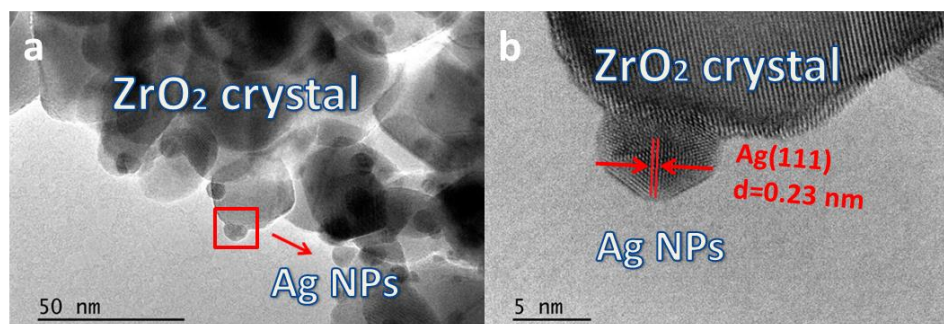
Figure 1. (a) TEM image of the Ag@ZrO$_2$ samples. (b) HR-TEM image of Ag particle indicated in part a (red square).

Ag NPs supported on zirconium oxide (Ag@ZrO$_2$) catalysts were prepared in the present study. The total metal amount of the catalyst was controlled at 3 wt%. The pattern of X-ray photoelectron spectroscopy (XPS) is shown in Figure 2. The binding energy peaks of Ag NPs at 374.2 eV and 368.2 eV can be attributed to the zero valence of Ag, thus the metallic state of Ag in NPs was confirmed.[17]
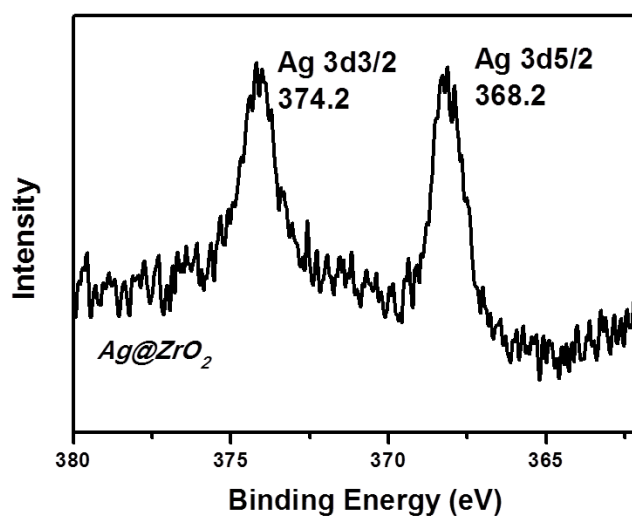
**Figure 2.** XPS profile of Ag species in the Ag NPs.

One of the important features of the photocatalyst is its light absorption property, which represents the light absorption ability of the catalyst. The diffuse reflectance UV-visible (DR-UV-vis) spectra of supported Ag NPs are shown in Figure 3. The light absorption peak of the Ag NPs is located at 392 nm which is attributed to the LSPR effect. The ZrO$_2$ support

exhibits negligible absorption of light with wavelengths above 400 nm, thus the support itself does not show any light absorption in the visible range. As a result, the absorption of the photocatalyst in the visible light range is due to Ag NPs, indicating that Ag NPs may have the potential to utilize the irradiation energy.
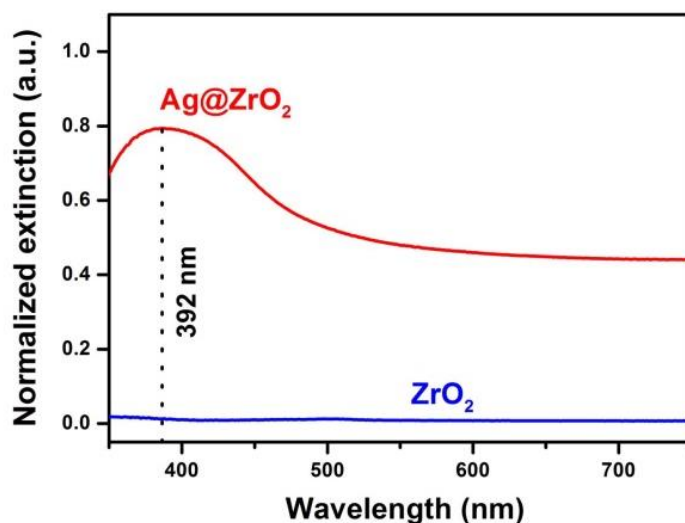
Figure 3. The normalized diffuse reflectance UV−visible (DR-UV−vis) spectra of the Ag@ZrO$_2$ catalyst.[19-20]

It can be seen from Figure 4 that the X-ray diffraction (XRD) patterns of the Ag@ZrO$_2$ photocatalysts. The diffraction peaks of all the two samples can be indexed to a monoclinic structure of the ZrO$_2$ crystal. The reflection peaks of Ag cannot be identified due to the low metal content (3 wt%). As a result, the loading of Ag NPs have no impact on the crystal structure of ZrO$_2$ support.[21]
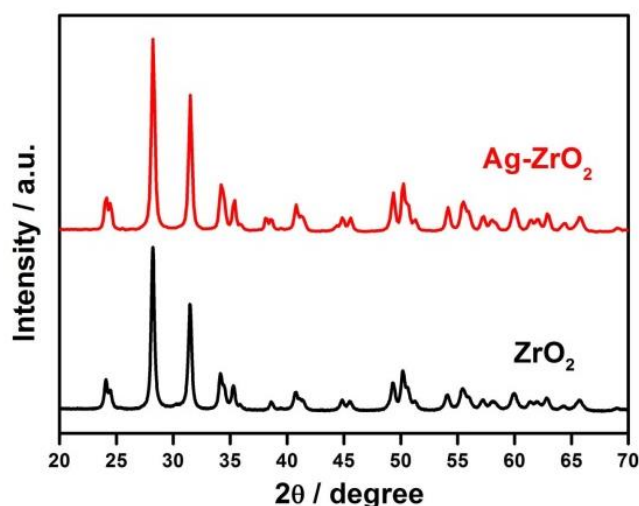
Figure 4. The XRD patterns of the photocatalysts.[22]

3.2 Photocatalytic Performance

Tables 1 and 2 show the photocatalytic performance of Ag NP catalysts for the redox reaction. Table 1 investigates the catalysis of Ag NPs for reduction of nitrobenzene to azobenzene under visible light irradiation. Isopropyl alcohol is both the reducing agent and solvent for this reaction. The results of reactions in dark at the same temperature are also provided for comparison. It can be seen that the conversion of reduction of nitrobenzene was 23% at 60 ℃ in dark, while it increased to 87% with the light irradiation. It can confirm that the Ag NPs exhibit excellent activity to this reaction in visible light irradiation as photocatalyst.

As shown in table 2, supported Ag NPs perform better in oxidation of benzyl alcohol to aldehyde. It can been seen from table 2 that the conversion was raised to 94% with the irradiation of visible light, while in dark the conversion was 0%. It can be confirmed that as photocatalyst, supported Ag NPs can both used in redox reaction, however better performance can be observed in oxidation of benzyl alcohol than in reduction of nitrobenzene. To investigate the general applicability of Ag NP in redox, a series of

differently substituted nitro compound and benzyl alcohol with different substance group were arranged. As shown in table 1 and table 2, the irradiation of visible light promoted the reaction rate in both of the reactions.

To further understand the contribution of light and verify the photocatalytic mechanism, the dependence of catalytic activity on light irradiance (intensity) and wavelength was investigated.

Table 1. Performance of Ag NPs supported on ZrO_2 for reduction of nitrobenzene:
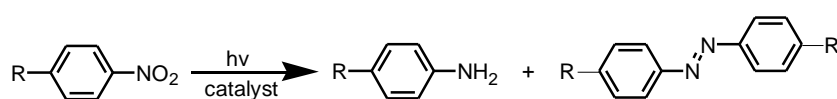
R	Light			Dark		
	Conversion (%)	Selectivity (%)		Conversion (%)	Selectivity (%)	
		Aniline	Azo		Aniline	Azo
H	87	25	75	23	54	46
Me	100	49	51	0	-	-
MeO	86	82	18	14	100	0
Cl	55	0	56	0	-	-
Br	50	100	0	0	-	-
I	100	100	0	0	-	-

Reaction condition: photocatalyst 50 mg, reactant 0.1 mmol, 2 mL IPA as solvent, 0.1 mmol KOH as base, 1 atm argon atmosphere, environment temperature 60 °C, the light intensity was $0.5W/cm^2$ and the reaction time was 6h. The conversions and selectivity were calculated from the product formed and the reactant converted measured by gas chromatography (GC).

Table 2. Performance of Ag NPs supported on ZrO_2 for oxidation of benzyl alcohol:
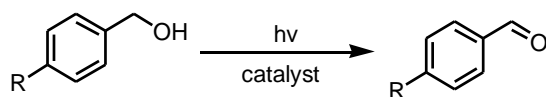
| R	Light		Dark	
	Conversion	Selectivity	Conversion	Selectivity
H	94	100	0	-
Cl	38	100	0	-
Me	47	100	0	-
MeO	100	100	0	-
NO$_2$	43	100	22	100

Reaction condition: photocatalyst 50 mg, 0.2 mmol BA, 2 mL toluene as solvent, 1 atm oxygen atmosphere, environment temperature 60 °C, the light intensity was 0.5W/cm^2, and the reaction time was 16 h. The conversions and selectivity were calculated from the product formed and the reactant converted measured by gas chromatography (GC).

3.3 Impact of Light Intensity and Wavelength

The positive relationship between light intensity and conversion was investigated and the results are shown in Figure 5.[23] The conversion in the dark was regarded as the contribution of the thermal effect, we conducted the reaction under different irradiance (from 0.5 to 1.0 W/cm^2) while all the other conditions were kept identical. We can see that the conversion increased with the increasing of light intensity. The contributions of irradiation to the conversion efficiency were calculated by subtracting the extent of conversion achieved in the dark from the overall extent of the irradiated system.[24] For example, in the reduction of nitrobenzene, the contribution of irradiation accounts for only 34% when the irradiation was 0.2 W/cm^2, while it increased to 81% with the irradiation of 0.6 W/cm^2. It shows that the contribution of irradiation effect is increasing with the raise of light intensities, this is due to the reason that with higher light intensity, large amount of light induced energetic electrons can be excited thus give higher reaction rate.
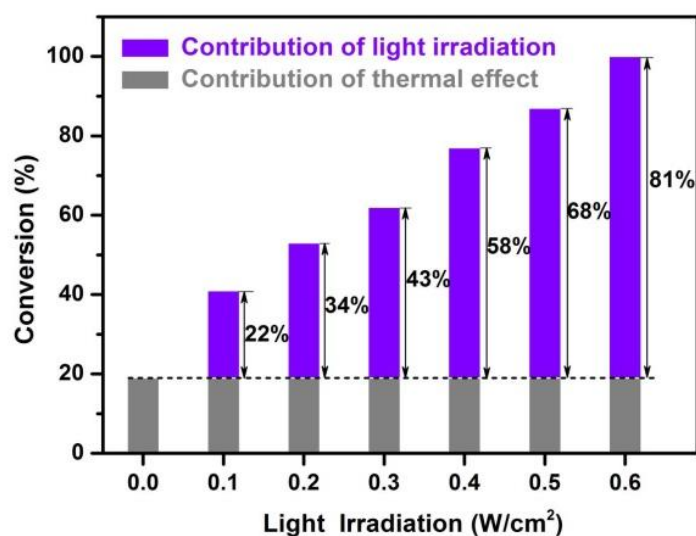
Figure 5. Dependence of the catalytic activity of Ag NPs for reduction of nitrobenzene on the intensity of light irradiation. The numbers with percentages show the contribution of the light irradiation effect. A photometer was used to measure the light intensity; the other experimental conditions were kept the same.
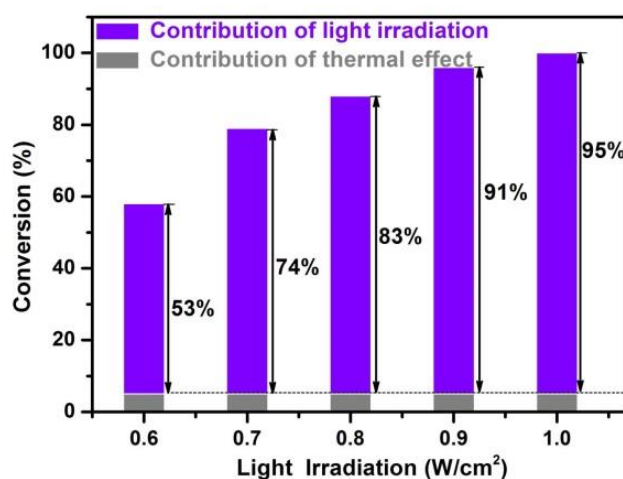
Figure 6. Dependence of the catalytic activity of Ag NPs for oxidation of benzylalcohol on the intensity of light irradiation. The numbers with percentages show the contribution of the light irradiation effect. A photometer was used to measure the light intensity; the other experimental conditions were kept the same.

Besides the intensity dependence, the impact of wavelength is another significant feature of the photocatalytic reactions. The action spectrum presents the mapping of the wavelength-dependent photocatalytic rate and the light extinction spectrum, which is a useful way to determine which wavelength of light can drive the reaction effectively.[25,26] We conducted the reduction of nitrobenzene over the Ag NPs as a model reaction. Five LED lamps with wavelengths of 400 ± 5, 470 ± 5, 530 ± 5, 590 ± 5, and 620 ± 5 nm were used as the light source. The reaction rate were calculated and presented as the apparent quantum efficiencies (AQEs).[27,28] The AQE was calculated using the relationship

$$\text{AQE (\%)} = [(Y_{light} - Y_{dark})/(\text{the number of incident photons})] \times 100$$

where Y_{light} and Y_{dark} are the amounts of products formed under light irradiation and dark conditions, respectively. The AQE for the two reactions were compared with the light absorption spectrum of Ag NPs respectively. It can be seen from Figure 7 and Figure 8 that the trend of AQE well matches with the light absorption curve of the Ag NPs. The action spectrum suggested that the enhancement of the catalytic performance was mainly due to the light absorption of the Ag NPs. The metal electrons gain sufficient energy from the LSPR effect under irradiation which can be then transfered into the reactant molecules absorbed on the metal surface to induce the reaction. As a reslut, it can be confirmed that it is Ag NPs that promote the reaction using visible light.
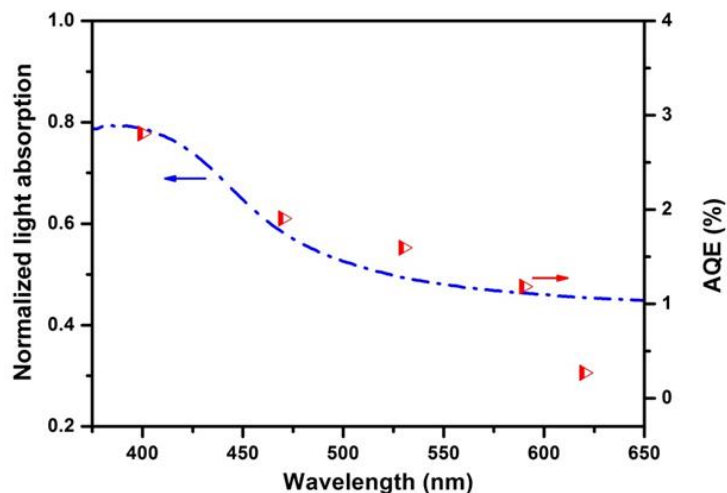
Figure 7. Photocatalytic action spectrum for the reduction of nitrobenzene using Ag@ZrO$_2$ photocatalyst. The light absorption spectrum (left axis) is the DR−UV/vis spectra of the supported Ag@ZrO$_2$ catalyst.
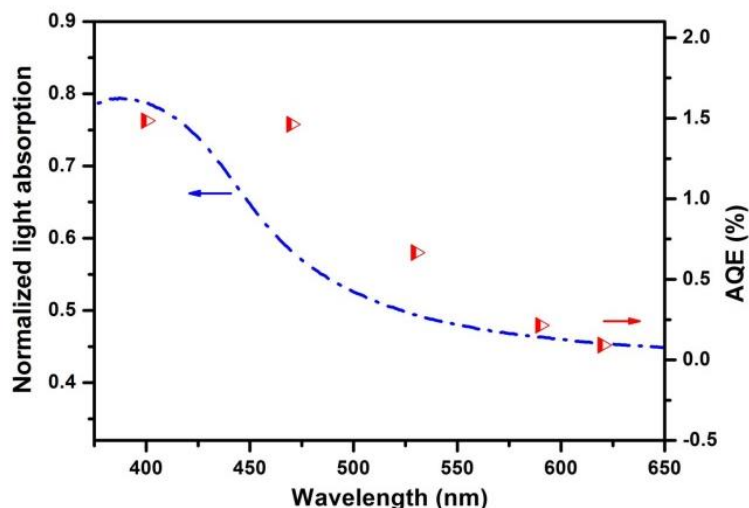
Figure 8. Photocatalytic action spectrum for the oxidation of benzylalcohol using Ag@ZrO$_2$ photocatalyst. The light absorption spectrum (left axis) is the DR−UV/vis spectra of the supported Ag@ZrO$_2$ catalyst.

Additionally, the apparent activation energy of the reaction can be calculated by the reaction rate at different temperatures using Arrhenius equation. To show the contribution of visible light, we calculate apparent activation energy for these two reactions respectively under light irradiation and in the dark, which is shown in Figure 9. It can be

seen that the apparent activation energy for reduction of nitrobenzene in the dark was 104.3 KJ/mol while only 32.2 KJ/mol for the reaction under illumination. The visible light irradiation reduced the activation energy of the reaction by 72.1 KJ/mol, which accounts for 69% of the apparent activation energy in the thermal reaction. The reduced apparent activation energy in irradiation indicates the contribution of light irradiation.[29]
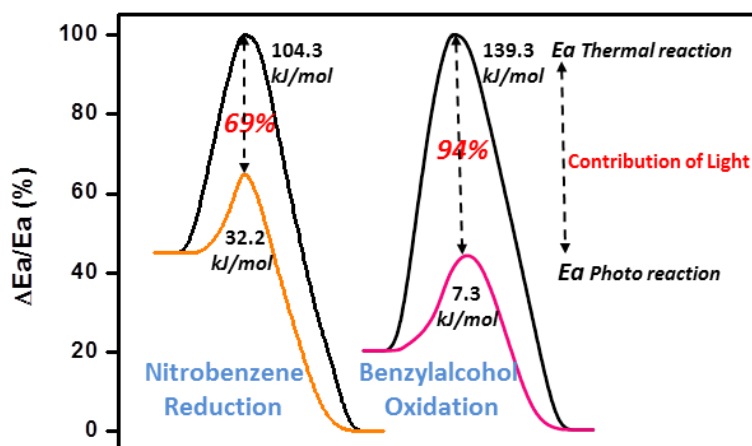
Figure 9. Apparent activation energies of nitrobenzene reduction and benaylaocohol oxidation calculated for the photoreaction and the reaction in the dark. The light intensity was 0.5 W/cm^2.

3.4 Impact of Temperature

Another important feature of the photocatalytic process on metal NP catalysts is that the photocatalytic activity of the NPs can be increased by elevating the reaction temperature.[24,30,31] For example as shown in Figure 10, the conversion of nitrobenzene reduction at 50℃ was 42%, whereas the conversion reached 100% when the temperature was ineased to 80℃(Figure 10, red dots). At a higher temperature, larger population of thermal activated electrons were generated with greater chance to surmount the activation barrier, thus it is easier for the activation of the reactions. Meanwhile, the vibrational states of the adsorbed molecules were excited by high reaction temperature and therefore the activation of substrate molecules is much easier. This theory can also

explain that the contribution decreases as the reaction temperature was raised. At low temperature, the thermal energy is insufficient to activate metal electrons to overcome the activation barrier therefore light excited electrons dominates the catalytic activity. In contrast, high reaction temperature can generates a remarkable amount of excited metal electrons capable of crossing activation barrier thus the contribution of light energy is suppressed.
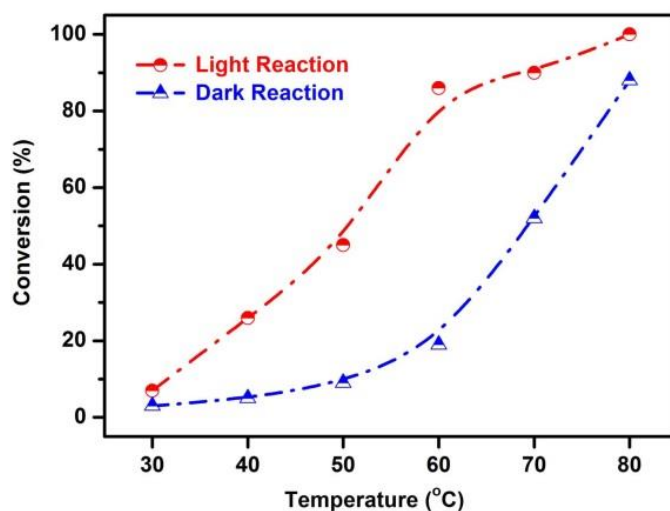
Figure 10. Dependence of catalytic activity on different reaction temperatures for reduction of nitrobenzene reaction under a thermal heating process in dark (blue) and the light irradiation process (red). The light intensity was 0.5 W/cm^2.
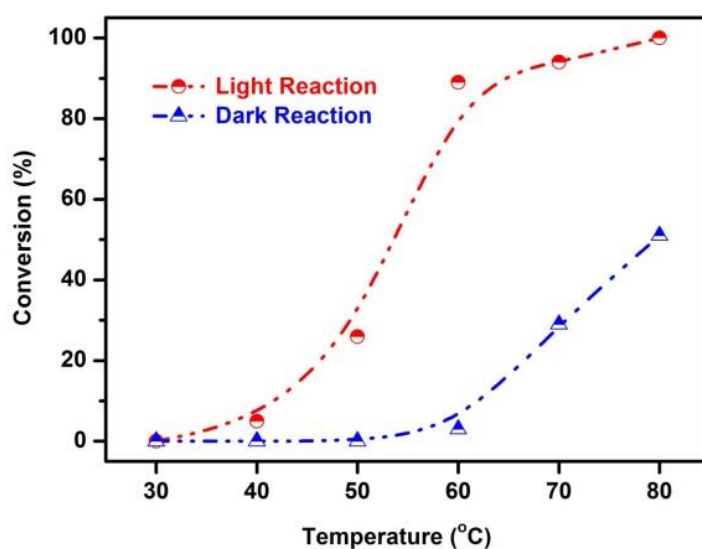
Figure 11. Dependence of catalytic activity on different reaction temperatures for oxidation of benzyl alcohol reaction under a thermal heating process in dark (blue) and the light irradiation process (red). The light intensity was 0.5 W/cm^2.

3.5 Proposed Mechanism

Table 3. Photocatalytic performance of pure Ag@ZrO$_2$ using various intermediates as reactant

| Entry	Substrate	Conv. (%)	Select. (%)		
			Aniline	Azo	Azoxy
1	⬡—NO$_2$	90	17	83	0
2[a]	⬡—NO	100	4	4	92
3[a]	⬡—NHOH	100	6	71	23
4[a]	⬡—NHOH + ⬡—NO	100	3	13	84
5	⬡—N$^+$(O$^-$)=N—⬡	16	0	100	0
6	⬡—N=N—⬡	0	-	-	-

Reaction condition: photocatalyst 50 mg, reactant 0.5 mmol, 3 mL IPA as solvent, 1 atm argon atmosphere, environment temperature 60°C, reaction time 16 h and the light intensity was 0.8 W/cm^2. The conversions and selectivity were analyzed by gas chromatography (GC). [a] reaction time 5 h.

In the Ag NPs catalyst's case, we observed that azobenzene cannot be further reduce to aniline, it leads to same conculsion of formation of aniline and azocompound are parallel reactions (entry 6, Table3). It was demonstrated Ag NPs cannot efficiently convert azoxybenzene into azobenzene (entry 5, Table 3), this phenomenon implies that in the reduction of nitrobenzene the great amount of azobenzene was not transfered from azoxybenzene but followes another pathway. On the other hand, when both nitrosobenzene and hydroxylamine was introduced into the reaction, we observed 84% yield of azoxybenzene (entry 4, Table 3). The reduction of nitrobenzene over Ag NPs catalyst cannot produce both nitrosobenzene and hydroxylamine otherwise azoxybenzene instead of azobenzene would have been observed. We seperately investigated the reduction of nitrosobenzene and hydroxylamine and found reduction of hydroxylamine gives similar selectivity as the reduction of nitrobenzene only with faster reaction rate (entries 1 and 3, Table 3), however adverse selectivity was observed with nitrosobenene (entry 2, Table 3). It illustrates the absence of nitrosobenzene as an intermediates in the reduction of nitrobenzene because if it exists stably in reaction system, azoxybenzene can be obtained as main product of coupling. Therefore, the complete reaction route of nitrobenzene reduction over Ag NPs catalyst is illuminated in Scheme 1.
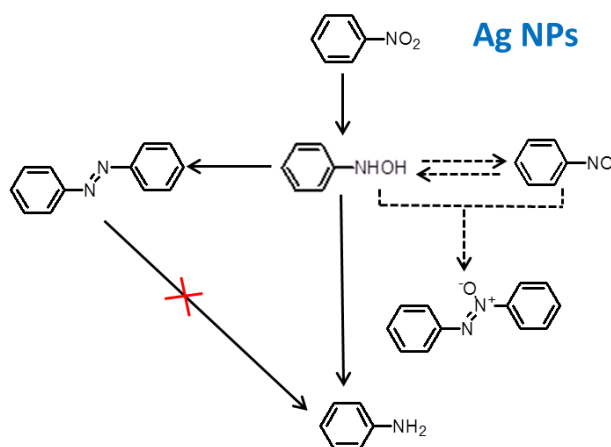
Scheme 1. Possible reaction pathways for the reduction of nitrobenzene with pure Ag NPs.

4. Conclusions

In conclusion, supported Ag NPs photocatalyst is a kind of efficient and green photocatalyst for redox reactions driven by light irradiation without intensive heating and pressured reagent. Meanwhile, the conversion of reactions can be enhanced with the rising of light irradiance and reaction temperature. The catalytic system provides us with a new direction for the application of Ag NP photocatalyst and also contribute to understanding the development of photocatalytic systems for more complex organic reactions driven by visible light under "green" mild conditions.

Reference list:

1. H. Tada, T. Ishida, A. Takao and S. Ito, *Langmuir*, 2004, **20**, 7898-7900.

2. K. Maeda, K. Teramura, D. Lu, T. Takata, N. Saito, Y. Inoue and K. Domen, *Nature,* 2006, **440**, 295-295.

3. R. Asahi, T. Morikawa, T. Ohwaki, K. Aoki and Y. Taga, *Science*, 2001, **293**, 269-271.

4. M. A. Garcia, J. Phys. D: *Appl. Phys.*, 2011, **44**, 283001.

5. X. Guo, C. Hao, G. Jin, H.-Y. Zhu and X.-Y. Guo, *Angew. Chem. Int. Ed.*, 2014, **126**, 2004-2008.

6. H. Zhu, X. Ke, X. Yang, S. Sarina and H. Liu, *Angew. Chem. Int. Ed.*, 2010, **122**, 9851-9855.

7. X. Ke, S. Sarina, J. Zhao, X. Zhang, J. Chang and H. Zhu, *Chem. Commun.,* 2012, **48**, 3509-3511.

8. Y. Wang, L. Sun and B. Fugetsu, *J. Mater. Chem. A,* 2013, **1**, 12536-12544.

9. O. V. Makarova, T. Rajh, M. C. Thurnauer, A. Martin, P. A. Kemme and D. Cropek, *Environ. Sci. Technol.*, 2000, **34**, 4797-4803.

10. A. M. Tafesh and J. Weiguny, *Chem. Rev.*, 1996, **96**, 2035-2052.

11. L. He, L.-C. Wang, H. Sun, J. Ni, Y. Cao, H.-Y. He and K.-N. Fan, *Angew. Chem. Int. Ed.*, 2009, **48**, 9538-9541.

12. R. Mantha, K. E. Taylor, N. Biswas and J. K. Bewtra, *Environ. Sci. Technol.*, 2001, **35**, 3231-3236.

13. D. I. Enache, J. K. Edwards, P. Landon, B. Solsona-Espriu, A. F. Carley, A. A. Herzing, M. Watanabe, C. J. Kiely, D. W. Knight and G. J. Hutchings, *Science*, 2006, **311**, 362-365.

14. K. R. Seddon and A. Stark, *Green Chem.*, 2002, **4**, 119-123.

15. J. R. Morones, J. L. Elechiguerra, A. Camacho, K. Holt, J. B. Kouri, J. T. Ramírez and M. J. Yacaman, *Nat. Nanotech.*, 2005, **16**, 2346.

16. M. R. Das, R. K. Sarma, R. Saikia, V. S. Kale, M. V. Shelke and P. Sengupta, *Colloids. Surf. B. Biointerfaces.*, 2011, **83**, 16-22.

17. J. Song and B. Kim, *Bioprocess. Biosyst. Eng.*, 2009, **32**, 79-84.

18. S. Pal, Y. K. Tak and J. M. Song, *Appl. Environ. Microbio.*, 2007, **73**, 1712-1720.

19. J. J. Mock, M. Barbic, D. R. Smith, D. A. Schultz and S. Schultz, *Journal. Chem. Phys.*, 2002, **116**, 6755-6759.

20. J.-Z. Guo, H. Cui, W. Zhou and W. Wang, *J. Photochem. Photobiol. A, Chem.*, 2008, **193**, 89-96.

21. G. R. Rao and H. R. Sahu, *J. Chem. Sci.*, 2001, **113**, 651-658.

22. S. Han, B. Jang, T. Kim, S. M. Oh and T. Hyeon, *Adv. Funct. Mater.*, 2005, **15**, 1845-1850.

23. Q. Xiao, E. Jaatinen and H. Zhu, *Chem. Asian. J.*, 2014, **9**, 3046-3064.

24. Q. Xiao, Z. Liu, A. Bo, S. Zavahir, S. Sarina, S. Bottle, J. D. Riches and H. Zhu, *J. Am. Chem. Soc.*, 2015, **137**, 1956-1966.

25. A. Tanaka, S. Sakaguchi, K. Hashimoto and H. Kominami, *ACS. Catal.*, 2013, **3**, 79-85.

26. E. Kowalska, R. Abe and B. Ohtani, *Chem. Commun.*, 2009, 241-243.

27. Q. Xiao, S. Sarina, E. Jaatinen, J. Jia, D. P. Arnold, H. Liu and H. Zhu, *Green Chem.*, 2014, **16**, 4272-4285.

28. Q. Xiao, S. Sarina, A. Bo, J. Jia, H. Liu, D. P. Arnold, Y. Huang, H. Wu and H. Zhu, *ACS. Catal.*, 2014, **4**, 1725-1734.

29. S. Sarina, E. R. Waclawik and H. Zhu, *Green Chem.*, 2013, **15**, 1814-1833.

30. S. Linic, P. Christopher and D. B. Ingram, *Nat. Mater.*, 2011, **10**, 911-921.

31. P. Christopher, H. Xin, A. Marimuthu and S. Linic, *Nat. Mater.*, 2012, **11**, 1044-1050.

Chapter 3:

Supported Ag-Cu Alloy Nanoparticles for Organic Synthesis under Visible Light Irradiation at Ambient Temperature

Introductory Remarks

In this chapter, we designed the Ag-Cu alloy nanoparticles as photocatalyst to utilize incident light energy to catalyze the chemical syntheses at ambient temperatures. As we know, Cu is active as catalyst in many thermal reactions; however the Cu NPs are easy to be oxidized, which is the limitation in the application of photocatalyst, although it exhibit absorption in visible light. To obtain stable metallic Cu NPs, we tried different ratios of Ag-Cu alloy NPs; finally the alloy NPs with mole ratio of 4-1 for Ag to Cu shows best stability. After obtain the stable Ag-Cu alloy NPs supported on ZrO_2, we used it in reduction of aromatic nitro compounds. Compared with pure Ag NPs photocatalyst, Ag-Cu alloy NPs shows different selectivity to the product – azoxy compounds, which is a very interesting phenomenon. Moreover, the wavelength of incident light also can influence the selectivity of product. To better understand the reaction pathway of this reaction catalyzed by Ag-Cu alloy NPs photocatalyst, we design a serious of intermediates as reactant to find out the reaction rout. This finding inspires further studies in change the reaction pathway by alloying another metal

as photocatlyst. Furthermore, we plan to find more application of this Ag-Cu alloy NPs photocatalyst.

Statement of Contribution of Co-Authors

Publication title and date of publication or status:

Selective reduction of nitroaromatics to azoxy compounds on supported Ag-Cu alloy

nanoparticles through visible light irradiation

Zhe Liu, Yiming Huang, Qi Xiao* and Huaiyong Zhu

Published on *Green Chemistry*, 2015

Article first published online: 8 Sep. 2015, DOI: 10.1039/C5GC01726B.

Contributor	Statement of contribution
Student Author. Zhe Liu Signature Date	Discovered the photocatalytic reaction, organized and designed the experiments, conducted the data collection, analyzed the data, proposed the reaction mechanism and wrote the manuscript
Yiming Huang	Analyzed data, offered interpretations, provided the detailed TEM analysis
Qi Xiao	Gave constructive suggestion on the reaction and polished the manuscript
Prof. Huaiyong Zhu	Proposed the idea

Principal Supervisor Confirmation

I have sighted email or other correspondence from all Co-authors confirming their certifying

authorship

QUT Verified Signature

HUAi YoNG ZHU   37/10/2015

Name   Signature   Date

Qi Xiao   QUT Verified Signature   1/06/2016

Yiming Huang   QUT Verified Signature   1/06/2016.

Article:

Selective reduction of nitroaromatics to azoxy compounds on supported Ag-Cu alloy nanoparticles through visible light irradiation

Zhe Liu, Yiming Huang, Qi Xiao* and Huaiyong Zhu

Abstract

The selective hydrogenation of aromatic nitrocompounds to their corresponding azoxy compounds is challenging in organic synthesis, which were typically performed under harsh reaction conditions. The core issue involved in this reduction is to finely control the product selectivity. Herein, we report an efficient photocatalytic process using supported silver-copper alloy nanoparticles (Ag-Cu alloy NPs) to selectively transform nitrobenzene to azoxybenzene by visible light irradiation under green mild reaction conditions. Ag-Cu alloy NPs can absorb visible light causing excited hot-electrons due to the localized surface plasmon resonance (LSPR) effect, and the excited electrons can activate the reactant molecule adsorbed on the NP surface to induce the reaction. The photocatalytic performance was affected by the ratio of Ag-Cu, and the catalyst with Ag-Cu molar ratio of 4-1 exhibited the optimal performance. Tuning the wavelength of incident light remarkably manipulate the product selectivity between azoxybenzene and aniline. Compared with pure Ag NPs, the alloying of Cu was found responsible for the product selectivity shifting from azobenzene to azoxybenzene. The reaction pathway was investigated to explain the selectivity difference and thus a tentative reaction pathway was proposed.

Introduction

The selective reduction of nitroaromatics is one of the most significant reactions in organic synthesis,[10, 11] because it produces important industrial intermediates such as

amines,[4] azo and azoxy compounds.[5] Among them, azo and azoxy compounds attract particular interest for their widely application in the production of dyes, agrochemical, and pharmaceuticals.[6-7] Therefore, a variety of reduction processes have been developed to catalyse this reaction selectively to obtain the desired products.[8-9] Generally, the stoichiometric amount of reducing agents such as pressured hydrogen as well as transition metal catalysts are demanded, which may result in undesired by–products and the uncontrollability of product selectivity.[10-11] Grirrane *et al.* demonstrated that supported gold nanoparticle (Au NP) catalyst is capable of catalysing the reduction of nitro aromatics to the corresponding azo compounds through a two-step process.[12] However, high reaction temperature, pressured hydrogen and oxygen gas were required, the harsh reaction conditions not only increase the energy consumption but also the safety risk. From the point of view of green chemistry, it would be a promising process to drive the reduction under mild reaction conditions through irradiation of visible light—the major component of abundant solar spectrum. In previous work, we have found that Au NPs supported on zirconium oxide (ZrO_2) effectively catalyse the reductive coupling of nitrobenzene to azo compound under ambient pressure at 40°C by visible light irradiation,[13] this is mainly due to the reason that Au NPs can strongly absorb visible light through the localized surface plasmon resonance (LSPR) effect.[14] The LSPR effect is the collective oscillation of conduction electrons in the metal NPs induced by the electromagnetic field of the incident light.[15] Through this process, the light excited electrons of NPs can gain the energy from light and activate reactant molecules adsorbed on metal surface and trigger chemical reactions.[16] Apart from Au NPs, silver (Ag) and copper (Cu) NPs also exhibits strong light absorption in the visible range.[17] It has been reported that supported Ag NPs can be used as efficient photocatalyst under ultraviolet (UV) and

visible light irradiation.[18-19] Very recently, Cu NPs supported on graphene were also been found to exhibit high photocatalytic activity for the reductive coupling of nitroaromatics to aromatic azo-compounds under irradiation of solar spectrum.[20] However, the main products in both of the Au and Cu NPs catalysed reaction systems were azo compounds, and azoxy compounds appear as the intermediates during these processes which is not easily controllable. We thus envision the design of a high-performance catalyst for the selective reduction of nitro compounds to azoxy compounds under much milder and greener reaction conditions driven by visible light irradiation.

In the present study, we reported the selective reduction of nitroaromatics to azoxy compounds on Ag-Cu alloy NPs under the irradiation of visible light. We successfully fabricated Ag-Cu alloy NPs with air stability by adjusting the Ag-Cu ratio. The Ag-Cu alloy NPs can efficiently drive the reduction of nitro aromatics and selectively yield azoxy compounds at moderate reaction temperature with the irradiation of visible light. From a green chemistry point of view, it would be a highly attractive and challenging goal to develop active, easily separable and reusable catalyst systems that can perform such desirable syntheses of aromatic azoxy compounds under more controlled, simplified, and greener conditions.

Results and discussion

Photocatalytic performance

Ag-Cu alloy NPs supported on ZrO_2 (Ag-Cu@ZrO_2) catalysts with different Ag:Cu ratio were prepared in the present study. The total metal amount (Ag+Cu) of the catalysts was maintained at 3 wt%. The photocatalytic reductions of nitrobenzene over Ag-Cu alloy NPs with different ratios under visible light irradiation were tested where

isopropyl alcohol was acting as both the solvent and reducing agent. The reactions isolated from light while other reaction condition remained unchanged were carried out for comparison. The results are summarized in Table 1. Monometallic Ag@ZrO$_2$ catalyst exhibited good catalytic activity with 90% conversion, while the control experiment in the dark only gave 25% conversion (entry 1). However, the main product was azobenzene (83%), and no azoxybenzene was detected. Cu@ZrO$_2$ catalyst gave poor activity for this reaction with only 38% conversion under irradiation (entry 2), this is probably due to the Cu NPs cannot be stabilized on the ZrO$_2$ surface, and the copper oxides on the surface strongly suppressed the catalytic activity. Interestingly, when using Ag-Cu alloy NPs as the catalyst, the main product selectivity was switched from azobenzene to azoxybenzene. The catalytic performance of alloy NPs was enhanced with higher Ag ratio, and the catalyst with Ag-Cu molar ratio of 4-1 exhibited the optimal performance (entry 3). Thus, the Ag-Cu (4-1) alloy @ZrO$_2$ was selected as the optimal catalyst for the following experiments. Further increasing the amount of Ag or Cu may form large amount of metal oxide species on the surface which significantly suppressed the catalytic performance. The different Ag-Cu ratio did not affect the reaction selectivity. The general applicability of Ag-Cu (4-1) alloy @ZrO$_2$ for the photocatalytic reduction of nitroaromatics with various functional groups was also investigated, the product selectivity can be maintained mainly at azoxy compounds and no azo product was detected (Table S1, ESI). These results confirmed that alloying Cu with Ag to form Ag-Cu alloy NPs can change the product selectivity for the reduction of nitroaromatic effectively at moderate conditions under visible light irradiation. Compared with some literature reported reaction conditions using Cu, Ag or Au catalysts for the reduction of nitrobenzene (Table 2), it can be seen that Ag-Cu alloy NPs can efficiently drive this reaction to obtain good azoxybenzene

yield under mild conditions through visible light irradiation. Thus, to the best of our knowledge, this is the first example of selective reduction of nitro aromatics to yield azoxy compounds at moderate reaction temperature driven by "green" solar energy.

**Table 1.** Activity test and catalyst screening for reduction of nitrobenzene.
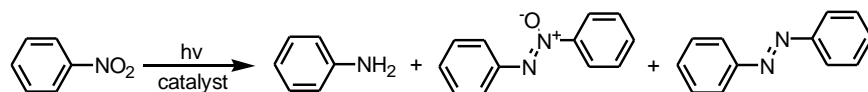
Entry	Ag:Cu[a]	Conv. (%) (dark)	Select. (%)			TON	TOF (h^{-1})
			Aniline	Azoxy	Azo		
1	Ag@ZrO$_2$	90 (25)	17	0	83	32	2.0
2	Cu@ZrO$_2$	38 (4)	12	76	12	8	0.5
3	4:1	96 (16)	14	86	0	32	2.0
4	1:1	74 (2)	18	82	0	21	1.3
5	1:4	57 (2)	16	83	1	14	0.9

Reaction condition: photocatalyst 50 mg, reactant 0.5 mmol, 3 mL isopropyl alcohol (IPA) as solvent, 0.15 mmol KOH as base, 1 atm argon atmosphere, reaction temperature 60°C, reaction time 16 h, and the light intensity was 0.8 W/cm^2. The conversions and selectivity were analysed by gas chromatography (GC). [a] Molar ratio. TON=[amount of nitrobenzene (mol) × conversion]/[amount of Ag (mol)+amount of Cu (mol)], TOF=TON/reaction time (h).

Table 2. Comparison of the reaction conditions and achieved conversion of metal catalysts reported in literatures for the reduction of nitrobenzene.

| Entry	Catalyst	Reaction conditions	Yield (%)		
			Aniline	Azobenzene	Azoxybenzene
1	Cu phthalocyanines [21]	70°C, 2h	93	-	-
2	Cu/HCOONH$_4$ [22]	120°C, 11h	86	-	-
3	Ag/TiO$_2$ [18]	1h	84	-	-
4	0.85 wt% Au/MgAl HT [23]	50°C, 3.5 h, 2 MPa H$_2$	-	98	-
5	Au/ZrO$_2$ [13]	40°C, 5h, visible light	-	99	-
6	Cu/graphene [20]	90°C, 5h, visible light	-	96	-
7	5.0 % Pd/Al$_2$O$_3$ [24]	65°C, 8h	-	-	44
8	Pd nanoparticle [25]	80°C, 24h	-	-	72
9	**Ag-Cu alloy@ZrO$_2$**	**60°C, 16h, visible light**	**-**	**-**	**75**
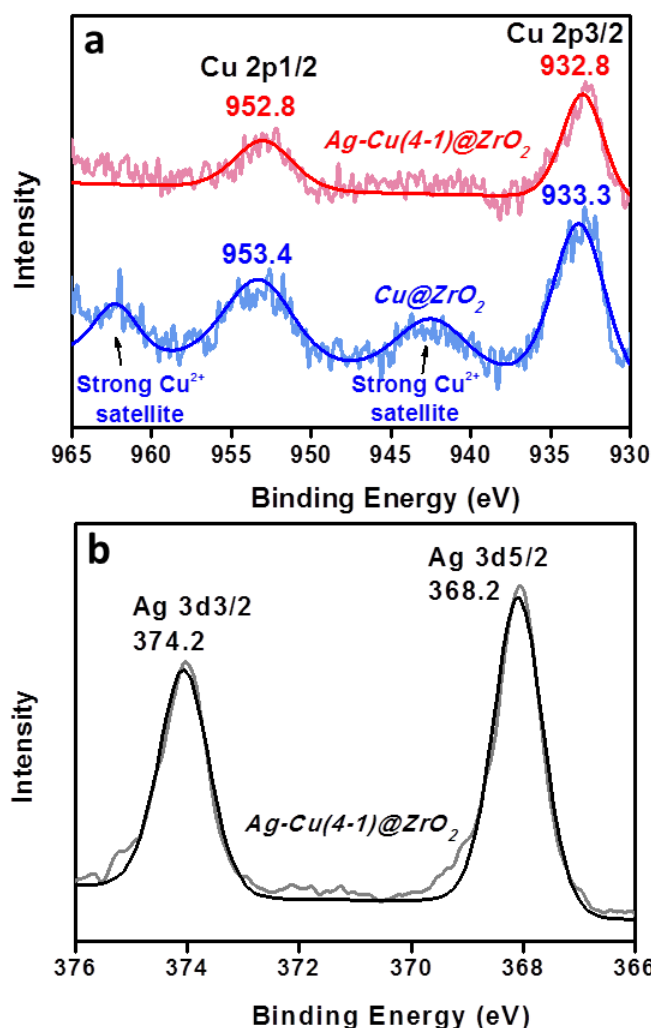
Figure 1. (a) XPS profile of Cu species in Ag-Cu (4-1)@ZrO$_2$ (red curve) and in Cu@ZrO$_2$ samples (blue curve). (b) XPS profile of Ag species in Ag-Cu (4-1)@ZrO$_2$ sample.

Catalyst characterization

Monometallic Cu NPs are unstable in the air, thus alloying Ag with Cu should be an effective approach to maintain its stabilization. To confirm the valence state of Cu species, the sample was tested by X-ray photoelectron spectroscopy (XPS) and results are shown in Figure 1. For comparison, the monometallic Cu sample was also tested. It can be seen from Figure 1a that the XPS spectra of Cu in Ag-Cu (4-1)@ZrO$_2$ and

Cu@ZrO$_2$ show much difference. First, two characteristic shake-up peaks at 942.7 eV and 962.2 eV can be observed in Cu@ZrO$_2$ sample (blue curve), which suggested that Cu(0) was oxidized to Cu(II) in the monometallic Cu sample. Thus, no further catalytic test was conducted with Cu@ZrO$_2$ sample due to it exists mainly as CuO. In the contrast, the shake-up peak disappeared in the Ag-Cu alloy sample (red curve), illustrating that Cu species existed in metallic state in alloy NPs when the Ag-Cu molar ratio was adjusted to 4-1.[26] On the other hand, as shown in Figure 1b, the binding energy peaks of Ag in alloy sample can be located at 368.2 eV and 374.2 eV attributed to the zero valence of Ag, thus the metallic state of Ag in bimetallic alloy can be confirmed.[27] These results suggested that we may use alloying effect to maintain the metal nanoparctiles' stability.

The representative transmission electron microscopy (TEM) images of the catalyst are shown in Figure 2. The Ag-Cu alloy NPs are well distributed on the ZrO$_2$ crystal surface (Figure 2a) with a mean particle size of 7 nm (Figure 2b). The high resolution (HR)-TEM image indicates that the crystal face of alloy nanoparticle is predominantly (111) face and the space of lattice fringe is 0.23 nm (Figure 2c). Figure 2d is a cross-sectional compositional line profile analysis of the energy dispersion X-ray (EDX) spectrum from TEM for a typical Ag-Cu (4-1) alloy NP, showing that the NP consists of both Ag and Cu elements distributed uniformly, which suggests that the two metals exist as binary alloy NPs in this sample. The composition of Ag and Cu elements in the alloy catalysts was also analyzed from the EDX spectrum (Figure 2e). The Ag/Cu ratio (4/1) is well matched with the initial experimental design. The appearance of both metals, Ag and Cu, in the elemental mapping from TEM also confirmed the alloy character of the bimetallic Ag-Cu catalyst (Figure 2f).
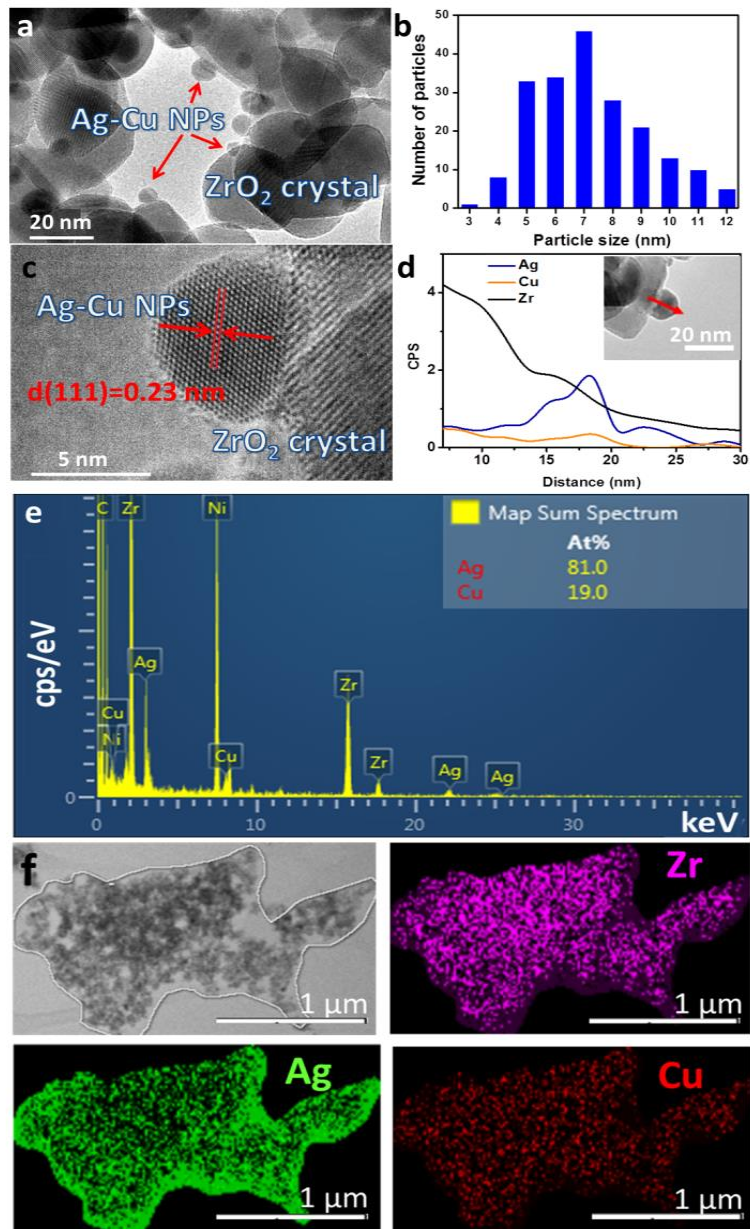
Figure 2. (a) TEM image of Ag-Cu (4-1)@ZrO_2 sample. (b) Particle size distribution of Ag-Cu (4-1)@ZrO_2 sample. (c) HR-TEM image of an Ag-Cu (4-1)@ZrO_2 particle. (d) The line profile analysis of Ag-Cu NP corresponding to the particle indicated by the red arrow in inset. (e) EDX spectrum of Ag-Cu (4-1)@ZrO_2 samples. (f) EDX mapping of Zr, Ag and Cu elements.

One of the important features of the photocatalyst is its light absorption property, which represents the light absorption ability of the catalyst. The diffuse reflectance

UV-visible (DR-UV-vis) spectra of supported Ag-Cu alloy NPs are shown in Figure 3. The light absorption peak of the Ag−Cu (4-1) NPs is located at 408 nm while the light absorption peak of pure Ag NPs is 392 nm which is attributed to the LSPR effect. The ZrO_2 support exhibits negligible absorption of light with wavelengths above 400 nm, thus the support itself does not show any light absorption in the visible range.[28] As a result, the absorption of the photocatalyst in the visible light range is due to the formation of Ag-Cu alloy NPs, indicating that the alloy NPs may have the potential to utilize the irradiation energy delivered by the wider range of solar spectrum.
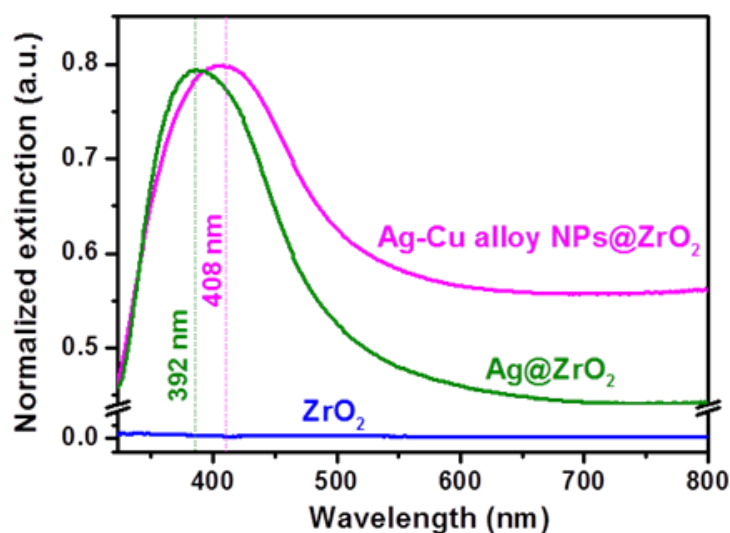
Figure 3. The normalized DR-UV-vis spectra of the Ag-Cu (4-1) @ZrO_2 catalyst, as well as its comparison with monometallic Ag@ZrO_2 and ZrO_2 support.

The X-ray diffraction (XRD) patterns of the Ag@ZrO_2 and Ag-Cu alloy@ZrO_2 photocatalysts are shown in Figure 4. It can be seen that the diffraction peaks of all the samples can be indexed to a monoclinic structure of the ZrO_2 crystal.[29] The reflection peaks of Ag and alloy cannot be identified due to the low metal content (3 wt%). As a result, the loading of alloy NPs have no impact on the crystal structure of ZrO_2 supporting material.
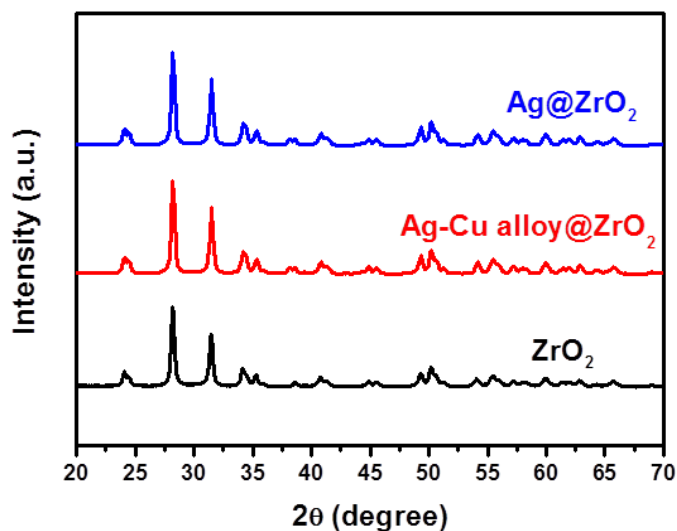
Figure 4. The XRD patterns of the photocatalysts.

Impact of wavelength and light intensity

To further understand the contribution of light and verify the photocatalytic mechanism, the dependence of catalytic activity on wavelength and light irradiance (intensity) was investigated. Action spectrum presents the mapping of the wavelength-dependent photocatalytic rate and the light extinction spectrum, which is a useful way to determe which wavelength of light can drive reaction effectively.[30-31] We conducted the reduction of nitrobenzene over Ag-Cu (4-1) alloy photocatalyst as model reaction. Five LED lamps with wavelengths of 400 ± 5, 470 ± 5, 530 ± 5, 590 ± 5, and 620 ± 5 nm were used as light source. The reaction rates were calculated and presented in apparent quantum yield (AQY).[32-33] The AQY for the reduction of nitrobenzene were compared with the light absoroption spectrum of Ag-Cu alloy NPs. It can be seen from Figure 5 that the trend of AQY well matches with the light absorption curve of the Ag-Cu alloy photocatalyst. The most significant enhancement of reaction rate was obseved at 400 nm, where LSPR peak of Ag-Cu alloy NPs located. The action spectrum suggested that the enhancement of the catalytic performance was mainly due to the light absorption of the alloy NPs. The metal electrons gain sufficient energy

from the LSPR effect under irradiation which can be then transfered into the reactant molecules absorbed on the metal surface to induce the reaction. Here, we can confirm that it is the alloy NPs that act as an antenna that harvest visible light enhancing the catalytic reaction activity.
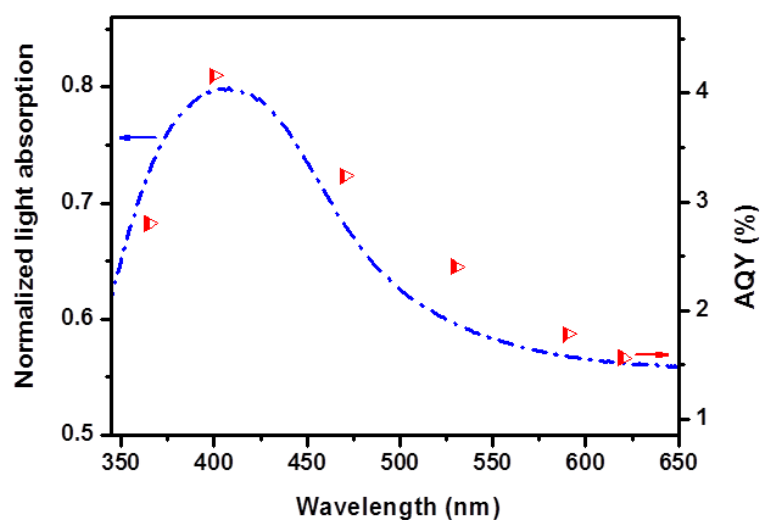
Figure 5. Photocatalytic action spectrum for the reduction of nitrobenzene using Ag-Cu(4-1)@ZrO$_2$ photocatalyst. The light absorption spectrum (left axis) is the DR−UV/vis spectrum of the supported Ag-Cu(4-1)@ZrO$_2$ catalyst.

Table 3. Performance of Ag-Cu (4-1)@ZrO$_2$ photocatalyst in nitrobenzene reduction with irradiation of different wavelengths.

Wavelength (nm)	AQY (%)	Conv. (%)	Select. (%)	
			Aniline	Azoxy
365	2.8	35	90	0
400	4.2	60	34	58
470	3.2	55	25	75
530	2.4	46	19	81

|				
590	1.8	38	16	84
620	1.6	35	11	89

Reaction condition: photocatalyst 50 mg, reactant 0.5 mmol, 3 mL IPA as solvent, 0.15 mmol KOH as base, 1 atm argon atmosphere, reaction temperature 70°C, reaction time 16 h, and the light intensity was 0.2 W/cm^2. The conversions and selectivity were analyzed by GC.

In addition to the reaction rate, we also found that the light wavelength can remarkablely affect the product selectivity as shown in Table 3. When shining by the light with the shortest wavelength (365 nm), the highest selectivity to aniline was obtained and the selectivity decreased with the increasing of wavelength. Such result illustrated that we can manipulate the selectivity of nitrobenzene reduction by the wavelength of incident light. The possible reason is that transfer of the energetic electrons to transform nitrobenzene to aniline require greater energy than that of azoxybenzene, light with shorter wavelengths can excite electron of metal to higher energy level and have greater chance to overcome the energy barrier to yield aniline.

Besides wavelength dependence, the impact of light intensity is another important feature of the photocatalytic reactions.[34] The dependence of catalytic activity on light irradiation intensity was investigated and the results is shown in Figure 6. The conversion in the dark was regarded as the contribution of thermal effect, we conducted the reaction under different irradiance (from 0.5 to 1.0 W/cm^2) while all the other reaction conditions were kept identical. We can see that the conversion increased with the incresing of light irridiance. The contributions of irradiation to the conversion efficiency were calculated by subtracting the extent of conversion achieved in the dark from the overall extent of the irradiated system.[35] To be more clear, the contribution of irradiation accounts for only 66% for the reaction when the irradiation was 0.5 W/cm^2,

while it increased to 83% with the irradiation of 1.0 W/cm^2. It shows that the contribution of irradiation effect is increasing with the raise of light intensities, this is due to the reason that with higher light intensity, larger amount of light energetic electrons can be excited thus give higher reaction rate.
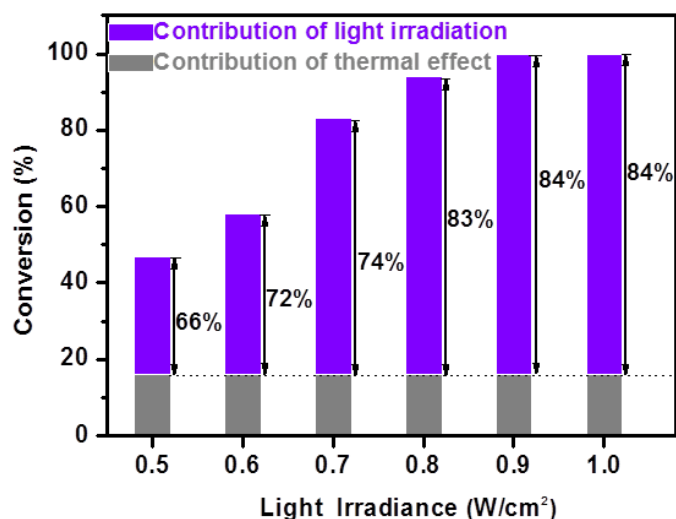
Figure 6. Dependence of the catalytic activity of Ag-Cu (4-1)@ZrO$_2$ for reduction of nitrobenzene on the intensity of light irradiation. The numbers with percentages show the contribution of the light irradiation effect. A photometer was used to measure the light intensity; the other experimental conditions were kept the same.

The relationship of reaction activity with the light irradiance and wavelength confirmed that the light excited energetic eletrons play the key role in photocatalysed reactions. The population of energetic electrons can be enhanced by applying higher light irradiance and turning the wavelength of irradiation.

Impact of temperature

Another important feature of the photocatalytic process on metal NP catalysts is that the photocatalytic activity of the NPs can be increased by elevating the reaction temperature.[36-37] As shown in Figure 7, higher reaction yield was achieved with the

temperature raising both under irradiation and in the dark. However, the contribution of light irradiation reduced with the rising of reaction temperature. For example, when at 50°C, the difference between the light reaction and dark reaction was 68% accounting for 97% of the total conversion, which decreased to 61% when the temperature was increased to 70°C. Under thermal heating conditions, the thermal activated electons of metal NPs can activate adsborbed moleculars and trigger the chemical reactions as well. At high reaction temperature, larger population of thermal activated electrons were generated with greater chance to surmount the activation barrier, thus it is easier for the activation of the reactions. Meanwhile, the vibrational states of the adsorbed molecules were excited by high reaction temperature and therefore the activation of substrate molecules is much easier.[35] This theory can also explain that the contribution decreases as the reaction temperature was raised. At low temperature, the thermal energy is insufficient to activate metal electrons to overcome the activation barrier therefore light excited electrons dominates the catalytic activity. In contrast, high reaction temperature can generates a remarkable amount of excited metal electrons capable of crossing activation barrier thus the contribution of light energy is suppressed.
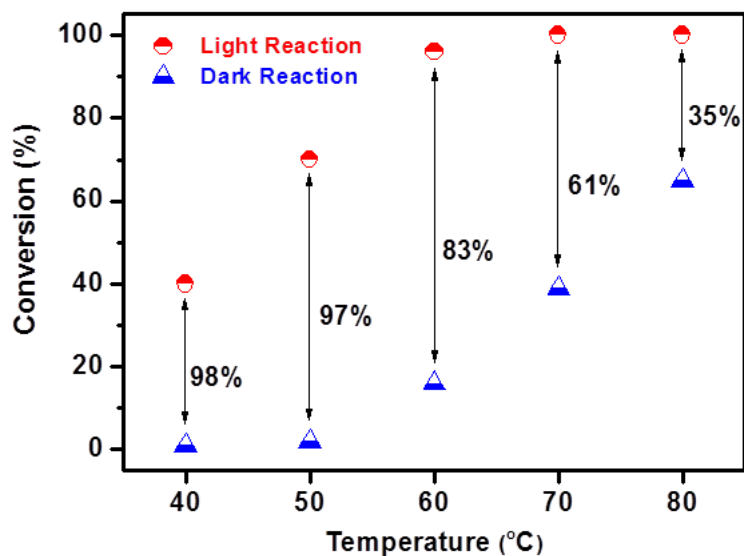
Figure 7. Dependence of catalytic activity on different reaction temperatures for reduciton of nitrobenzene under a thermal heating process in dark (blue triangles) and the light irradiation process (red circles). The light intensity was 0.8 W/cm^2.

The effect of temperature on the product selectivity was also investigated. As shown in Table 4, with the raising of temperature, we did not obtain any siginificant changing of product selectivity. It can be concluded that temperature has limited influence on selectivity of nitrobenzene redcution compared with that of light wavelength in this reaction.

Table 4. Performance of Ag-Cu (4-1)@ZrO$_2$ photocatalyst in nitrobenzene reduction at different temperatures.

Temp (°C)	Conv. (%)	Select. (%)	
		Aniline	Azoxy
40	40	27	73
50	70	21	78

60	96	14	86
70	100	11	85
80	100	13	87

Reaction condition: photocatalyst 50 mg, reactant 0.5 mmol, 3 mL isopropyl alcohol (IPA) as solvent, 0.15 mmol KOH as base, 1 atm argon atmosphere, reaction time 16 h, and the light intensity was 0.8 W/cm^2. The conversions and selectivity were analyzed by GC.

Additionally, the apparent activation energy of the reaction can be calculated by the reaction rate at different temperatures using Arrhenius equation. We conducted the reduction of nitrobenzene at diferent temperatures: 30°C, 40°C, 50°C, 60°C, 70°C and 80°C both under irradiation and in the dark (thermal process). The apparent activation energy of light reaction and dark reaction are shown in Figure 8, it can be seen that the apparent activation energy for reduction of nitrobenzene in the dark is 104.4 kJ mol^{-1} while only 20.4 kJ mol^{-1} for the reaction under irradiation. The visible light irradiation reduced the activation energy of the reaction by 80 kJ mol^{-1}, which accounts for 80.4 % of the apparent activation energy in the thermal reaction. The reduced apparent activation energy in irradiation indicates the contribution of light irradiation.[38]
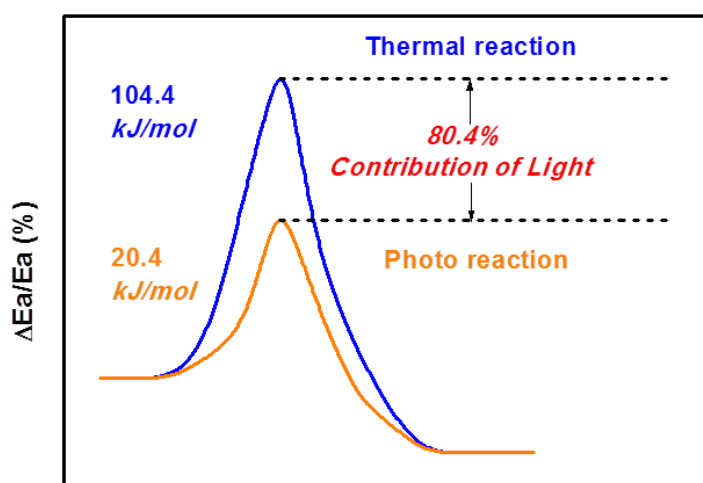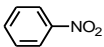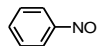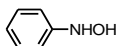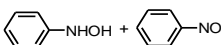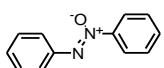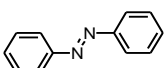
Figure 8. Apparent activation energies of nitrobenzene reduction calculated for the photoreaction and the reaction in the dark.

Proposed mechanism

A widely accepted mechanism for the reduction of nitrobenzene was proposed by Haber in 1898 that nitro group stepwise reduced to aniline through nitroso- and hydroxylamine, additionlay hydroxylamine is an highly active intermediate causing the yield of azoxy and azo compounds,[39] the further reduction of azo compounds results in the hydroazo compounds which is eventually transformed into aniline.[40-41]

Table 5. Photocatalytic performance of Ag-Cu (4-1)@ZrO_2 using various intermediates as reactant.

Entry	Substrate	Conv. (%)	Select. (%)		
			Aniline	Azo	Azoxy
1	phenyl-NO_2	96	14	0	86
2[a]	phenyl-NO	100	8	1	91
3[a]	phenyl-NHOH	100	29	9	61
4[a]	phenyl-NHOH + phenyl-NO	100	6	9	85
5	azoxybenzene	0	-	-	-
6	azobenzene	trace	-	-	-

Reaction condition: photocatalyst 50 mg, reactant 0.5 mmol, 3 mL IPA as solvent, 1 atm argon atmosphere, environment temperature 60°C, reaction time 16 h and the light intensity

was 0.8 W/cm^2. The conversions and selectivity were analysed by gas chromatography (GC).

[a] reaction time 5 h.

Scheme 1. Possible reaction pathways for the reduction of nitrobenzene with Ag-Cu alloy NPs in the irradiation of visible light.

In this study, the fact that only azoxybenzene was obtained when using Ag-Cu Alloy NPs catalyst indicates a different reaction pathway regarding to the alloying of Cu and Ag (entry 1, Table 5.). First of all, the reduction of nitrobenzene over Ag-Cu alloy NPs produce azoxybenzene with minor aniline without other intermediates being detected. To further understand reaction route with Ag-Cu alloy NPs catalyst, several intermediates such as nitrosobenzene, hydroxylamine and azobenzene were used as substrates for the redcution to gain some insight into the reaction pathways.

In the Ag-Cu alloy NPs catalysed reaction system, trace aniline was obatined when using azoxybenzene and azobenzene as substrate (entries 5 and 6, Table 5.) indicating the azoxybenzene through azobenzene to aniline route is unfavorable. Therefore, it can be concluded the formation of aniline and azo-compound are parallel reactions. Compared with nitrobenzene, the reduction of nitrosobenzene and hydroxylamine is much faster. It is worth noticing that hydroxylamine gave greater yield to aniline than

nitrobenzene and nitrosobenzene indicating its responsible to the direct production of aniline (entries 2 and 3, Table 5). When two intermediates were used togther as the substrate, the similar selectivity to that of nitrobenzene was observed (entry 4, Table 5.). Hence, we proposed the reaction mechanism as shown in Scheme 1, Ag-Cu alloy NPs can catalyse the reduction of nitrobenzene through the coupling of nitrosobenzene and hydroxylamine, instead of futher reducing to azobenzene or aniline. The Ag-Cu alloy NPs cannot transfer azoxybenzene into azobenzene possiblely due to the limited reductive ability.

Recycle of photocatalyst

The reusability is a significant character of heterogeneous catalyst.[42] Therefore we performed the recycle experiments for the catalyst. The catalyst was reused for 10 times to test the activity and the other reaction conditions were kept identical. After each reaction cycle, the catalyst was separated by centrifugation, washed with ethanol twice, and then dried for subsequent reactions. As shown in Figure 9, the catalyst was recycled for 10 times with less than 20% reduction of the catalytic activity. Noticeably, the selectivity to azoxybenzene can be still maintained above 70%. The observed slightly loss in catalytic activity was possibly due to the leaching of the NPs or the loss of NPs during washing after each catalytic run. To further confirm the heterogeneous nature of the alloy catalyst, we tested the amount of Ag and Cu in the reaction supernatant liquid by Inductively coupled plasma-atomic emission spectroscopic (ICP-AES) analysis, the amount of leaching was detectable (<10 ppm), but there was very little leaching of Ag during the reaction and the amount of the leached Cu decreased apparently with the recycle times. Thus, overall it is evident that the reaction was predominately catalysed by the supported heterogeneous alloy NPs. The TEM image indicates that the Ag-Cu alloy NPs still distributed evenly after several times reactions,

and the mean particle size remained 7 nm (Figure 10). These results confirmed that the Ag-Cu alloy NPs are stable and resuable photocatalyst for the reduction of nitrobenzene.
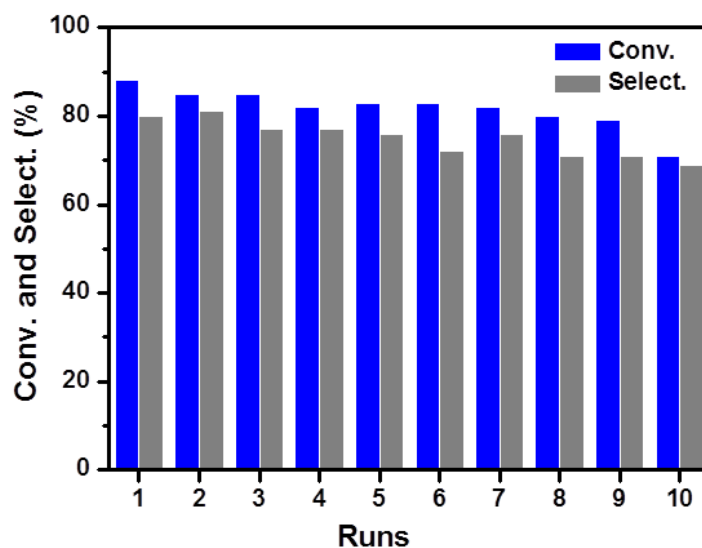
Figure 9. The reusability of the Ag-Cu alloy NPs for reduction of nitrobenzene under visible light irradiation. The selectivity is to azoxybenzene. Reaction conditions: photocatalyst 50 mg, reactant 0.5 mmol, 3 mL isopropyl alcohol (IPA) as solvent, 0.15 mmol KOH as base, 1 atm argon atmosphere, reaction temperature 60°C, reaction time 16 h and the light intensity was 0.8 W/cm^2. The conversions and selectivity were analysed by gas chromatography (GC).
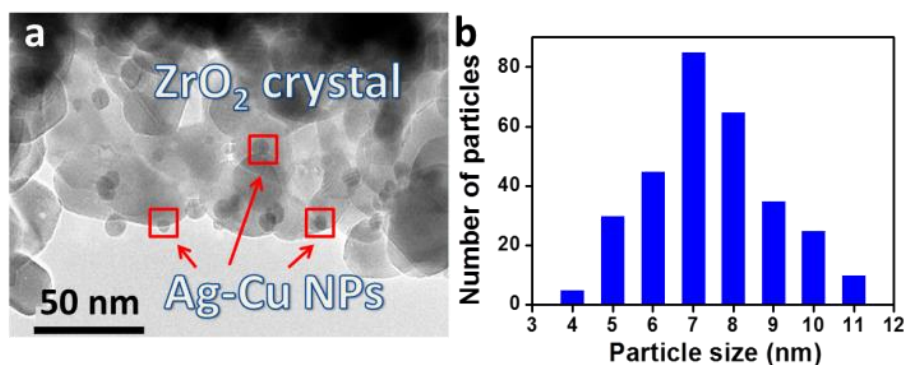
Figure 10. (a) TEM image of Ag-Cu (4-1)@ZrO$_2$ sample after 10 catalytic cycles. (b) Particle size distribution of Ag-Cu (4-1)@ZrO$_2$ sample after 10 catalytic cycles.

Conclusion

In Summary, a green photocatalysis process for selective reduction of nitro compounds to azoxy compounds, driven by light irradiation without intensive heating and pressured reagent, can be achieved using Ag-Cu alloy NP catalyst prepared simply by alloying small amount of Cu into Ag NPs. The alloying of Cu into Ag NPs can maintain the azoxy compounds as main product, which is not easily controllable when using pure Ag NPs as catalyst. The catalyst with Ag-Cu ratio 4:1 exhibited the best photocatalytic performance and maintained stability in air. The selectivity to azoxybenzene and aniline can be controlled by turning the wavelength of irradiation. Meanwhile, the conversion of reactions can be enhanced with the rising of light irradiance and reaction temperature. The solid catalyst can be recycled and reused for several runs without significantly losing activity. The catalytic system provides us with a new direction for the application of alloy NP photocatalyst and also contribute to understanding the development of photocatalytic systems for more complex organic reactions driven by visible light under "green" mild conditions.

Experimental section

Catalysts preparation

3 wt% Ag-Cu alloy NPs on ZrO_2 (Ag-Cu alloy @ZrO_2) with different ratios were prepared by the impregnation−reduction method. For example, Ag-Cu alloy NPs of molar ratio 4:1 was prepared as follow, $AgNO_3$ (82.3 mg) and $Cu(NO_3)_2 \cdot 6H_2O$ (29.3 mg) was dissolved into 60 mL deionized water, to the above solution ZrO_2 nanopowder (2.0 g) was dispersed followed by adding 20 mL lysine aqueous (0.01 M) solution. The mixture was kept under magnetic stirring at room temperature for 20 min. To this suspension, 10 mL of freshly prepared aqueous $NaBH_4$ (0.35 M) solution was

added dropwise. The mixture was aged for 24 h, and then the precipitate was separated by centrifugation, washed with water (three times) and ethanol (once), and dried at 60°C in vacuum for 24 h. The collected powder was used directly as catalyst. Other alloy catalysts with different Ag-Cu ratio, as well as NPs of pure Ag on the ZrO_2 support, were prepared via a similar method but using different amount of quantities.

Catalysts characterization

The morphology study of catalysts was carried out on a JEOL 2100 transmission electron microscopy (TEM) equipped with a Gatan Orius SC1000 CCD camera, with an accelerating voltage of 200 kV and nickel grids were used as the supporting film. Scanning electron microscope (SEM) imaging, elemental mapping and EDX were performed using a ZEISS Sigma SEM at accelerating voltages of 20 kV. Diffuse reflectance UV-visible spectra of the sample catalysts were examined by a Varian Cary 5000 spectrometer with $BaSO_4$ as a reference. X-ray photoelectron spectroscopy (XPS) data was acquired using a Kratos Axis ULTRA X-ray Photoelectron Spectrometer incorporating a 165 mm hemispherical electron energy analyser. The incident radiation was Monochromatic Al Kα X-rays (1486.6 eV) at 225W (15 kV, 15 ma). Narrow high-resolution scans were run with 0.05 ev steps and 250 ms dwell time. Base pressure in the analysis chamber was $1.0x10^{-9}$ torr and during sample analysis $1.0x10^{-8}$ torr. X-ray diffraction (XRD) patterns of the sample powders were collected using a Philips PANalytical X'pert Pro diffractometer. Cu Kα radiation ($λ= 1.5418$ Å) and a fixed power source (40 kV and 40 mA) were used. Inductively coupled plasma-atomic emission spectroscopic (ICP-AES) analysis was performed using a Perkin Elmer 8300DV ICP fitted with an ESI SC-4DX auto-sampler and PrepFAST 2 sample handling unit for online internal standardisation and auto-dilution of samples and

calibration standards. Nitric acid, purified by sub-boiling distillation was used for the preparation of all standards and blank solutions used throughout the analysis.

Activity test

In a typical activity test, a 20 mL Pyrex glass tube was used as the reaction vessel. The vessel containing reactants and catalyst was irradiated with visible light using a halogen lamp (from Nelson, wavelength in the range of 400−750 nm) under magnetic stirring; the irradiance was measured to be 0.8 W/cm^2. The reaction temperature was carefully controlled with an air conditioner attached to the reaction chamber. The reactions in the dark were conducted using an oil bath placed above a magnetic stirrer to maintain the reaction temperature the same to corresponding reactions with light illuminations; reaction tubes were wrapped with aluminum foil to avoid exposure to light. At given irradiation time intervals, 0.5 mL aliquots were collected, the catalyst particulates was removed by a Millipore filter (pore size 0.45 μm). The liquid−phase products were analyzed by gas chromatography (GC) technique (Agilent 6890) with a HP−5 column to monitor the change in the concentrations of reactants and products. An Agilent HP5973 mass spectrometer was used to identify the product.

In action spectrum experiments, light emission diode (LED) lamps (Tongyifang, Shenzhen, China) with wavelengths 360±5 nm, 400±5 nm, 470±5 nm, 530±5 nm, 590±5 nm and 620±5 nm were used as light source. The reaction temperature was controlled with oil bath with all the other reaction conditions identical to those of typical reaction procedures. The apparent quantum yield (AQY) was calculated as follow: apparent quantum yield = [(M_{light}–M_{dark})/N_p] × 100%, where M_{light} and M_{dark} are the molecules of products formed under irradiation and dark conditions respectively, M = mole number of the reactant × conversion × 6.02 × 10^{23} (Alvarado constant). N_p is the number of photons involved in the reaction. N_p = E_{total}/E_1, E_{total}

(the total energy involved in the reaction irradiation) = intensity × light spot area × reaction time, E_1 (the energy of one photon) = h × c / L (h is Planck constant, c is light speed, L is wavelength of the LED light).

References list

1. M. Tafesh and J. Weiguny, *Chem. Rev.*, 1996, **96**, 2035-2052.

2. L. He, L.-C. Wang, H. Sun, J. Ni, Y. Cao, H.-Y. He and K.-N. Fan, *Angew. Chem. Int. Ed.*, 2009, **48**, 9538-9541.

3. R. Mantha, K. E. Taylor, N. Biswas and J. K. Bewtra, *Environ. Sci. Tech.*, 2001, **35**, 3231-3236.

4. A.-J. Wang, H.-Y. Cheng, B. Liang, N.-Q. Ren, D. Cui, N. Lin, B. H. Kim and K. Rabaey, *Environ. Sci. Tech.*, 2011, **45**, 10186-10193.

5. F. Figueras and B. Coq, *J. Mol. Catal. A: Chem.*, 2001, **173**, 223-230.

6. J. M. Joseph, H. Destaillats, H.-M. Hung and M. R. Hoffmann, *J. Phys. Chem. A*, 2000, **104**, 301-307.

7. S. S. Acharyya, S. Ghosh and R. Bal, *ACS Sustain. Chem. Eng.*, 2014, **2**, 584-589.

8. Agrawal and P. G. Tratnyek, *Environ. Sci. Tech.*, 1996, **30**, 153-160.

9. Y. Moglie, C. Vitale and G. Radivoy, *Tetrahedron Lett.*, 2008, **49**, 1828-1831.

10. K. Ohe, S. Uemura, N. Sugita, H. Masuda and T. Taga, *J. Org. Chem.*, 1989, **54**, 4169-4174.

11. Roucoux, J. Schulz and H. Patin, *Chem. Rev.*, 2002, **102**, 3757-3778.

12. Grirrane, A. Corma and H. García, *Science*, 2008, **322**, 1661-1664.

13. H. Zhu, X. Ke, X. Yang, S. Sarina and H. Liu, *Angew. Chem. Int. Ed.*, 2010, **49**, 9657-9661.

14. S. Sarina, H. Zhu, E. Jaatinen, Q. Xiao, H. Liu, J. Jia, C. Chen and J. Zhao, *J. Am. Chem. Soc.*, 2013, **135**, 5793-5801.

15. H. Zhu, X. Chen, Z. Zheng, X. Ke, E. Jaatinen, J. Zhao, C. Guo, T. Xie and D. Wang, *Chem. Commun.*, 2009, **48**, 7524-7526.

16. S. Linic, U. Aslam, C. Boerigter and M. Morabito, *Nat. Mater.*, 2015, **14**, 567-576.

17. J. C. Scaiano, K. G. Stamplecoskie and G. L. Hallett-Tapley, *Chem. Commun.*, 2012, **48**, 4798-4808.

18. H. Tada, T. Ishida, A. Takao and S. Ito, *Langmuir*, 2004, **20**, 7898-7900.

19. X. Chen, Z. Zheng, X. Ke, E. Jaatinen, T. Xie, D. Wang, C. Guo, J. Zhao and H. Zhu, *Green. Chem.*, 2010, **12**, 414-419.

20. X. Guo, C. Hao, G. Jin, H.-Y. Zhu and X.-Y. Guo, *Angew. Chem. Int. Ed.*, 2014, **53**, 1973-1977.

21. U. Sharma, P. Kumar, N. Kumar, V. Kumar and B. Singh, *Adv. Synth. Catal.*, 2010, **352**, 1834-1840.

22. Saha and B. Ranu, *J. Org. Chem.*, 2008, **73**, 6867-6870.

23. X. Liu, H.-Q. Li, S. Ye, Y.-M. Liu, H.-Y. He and Y. Cao, *Angew. Chem. Int. Ed.*, 2014, **53**, 7624-7628.

24. Morales-Guio, I. Yuranov and L. Kiwi-Minsker, *Top. Catal.*, 2014, **57**, 1526-1532.

25. L. Hu, X. Cao, L. Shi, F. Qi, Z. Guo, J. Lu and H. Gu, *Org. Lett.*, 2011, **13**, 5640-5643.

26. J. P. Espinós, J. Morales, A. Barranco, A. Caballero, J. P. Holgado and A. R. González-Elipe, *J. Phys. Chem. B*, 2002, **106**, 6921-6929.

27. M. Liu and W. Chen, *Nanoscale*, 2013, **5**, 12558-12564.

28. Marimuthu, J. Zhang and S. Linic, *Science*, 2013, **339**, 1590-1593.

29. G. Ranga Rao and H. R. Sahu, *J. Chem. Sci.*, 2001, **113**, 651-658.

30. Tanaka, S. Sakaguchi, K. Hashimoto and H. Kominami, *ACS Catal.*, 2013, **3**, 79-85.

31. E. Kowalska, R. Abe and B. Ohtani, *Chem. Commun.*, 2009, **2**, 241-243.

32. Q. Xiao, S. Sarina, E. Jaatinen, J. Jia, D. P. Arnold, H. Liu and H. Zhu, *Green. Chem.*, 2014, **16**, 4272-4285.

33. Q. Xiao, S. Sarina, A. Bo, J. Jia, H. Liu, D. P. Arnold, Y. Huang, H. Wu and H. Zhu, *ACS Catal.*, 2014, **4**, 1725-1734.

34. Q. Xiao, E. Jaatinen and H. Zhu, *Chem. Asian. J.*, 2014, **9**, 3046-3064.

35. Q. Xiao, Z. Liu, A. Bo, S. Zavahir, S. Sarina, S. Bottle, J. D. Riches and H. Zhu, *J. Am. Chem. Soc.*, 2015, **137**, 1956-1966.

36. S. Linic, P. Christopher and D. B. Ingram, *Nat. Mater.*, 2011, **10**, 911-921.

37. P. Christopher, H. Xin, A. Marimuthu and S. Linic, *Nat. Mater.*, 2012, **11**, 1044-1050.

38. S. Sarina, E. R. Waclawik and H. Zhu, *Green. Chem.*, 2013, **15**, 1814-1833.

39. K. Möbus, D. Wolf, H. Benischke, U. Dittmeier, K. Simon, U. Packruhn, R. Jantke, S. Weidlich, C. Weber and B. Chen, *Top. Catal.*, 2010, **53**, 1126-1131.

40. Corma, P. Concepción and P. Serna, *Angew. Chem. Int. Ed.*, 2007, **46**, 7266-7269.

41. H.-U. Blaser, *Science*, 2006, **313**, 312-313.

42. Y. Zhang, Q. Xiao, Y. Bao, Y. Zhang, S. Bottle, S. Sarina, B. Zhaorigetu and H. Zhu, *J. Phys. Chem. C*, 2014, **118**, 19062-19069.

Chapter 4:

Conclusion and Future Work

Conclusion:

In this thesis, Ag NP and Ag-Cu alloy NP photocatalysts have been developed and used for selective redox reactions under visible light irradiation:

In Chapter 2, a stable, inexpensive, and reusable Ag NPs supported on ZrO_2 catalyst exhibit high activity and product selectivity for the redox reactions. The Ag NP photocatalyst shows a favourable activity and high selectivity on reduction of aromatic nitro compound to azo compounds and oxidation of aromatic alcohol compounds to aromatic aldehyde compounds under light irradiation and moderate temperature. The LSPR absorption of Ag NPs played an important role in visible light absorption, tuning light intensity and wavelength can obtain different reaction activity.

This study provides a general guiding principle for determing the applicability of Ag photocatalysts as well as a inspiration for designing suitable photocatalysts made from Ag alloyed with other transition metals.

In Chapter 3, we extended the study on Ag NP photocatalyst to Ag-Cu alloy NP photocatalysts, and the Ag-Cu alloy NPs can drive reduction of nitroaromatics to azoxy compounds under visible light irradiation in a different from the Ag NP photocatalyst. The photocatalytic reaction pathway can be finely tuned by addition small amount of Cu into Ag, which maintains Cu's ability on the surface and keep high catalytic activity as well.

In conclusion, the catalytic system destribed here may present a new strategy towards the development of new heterogeneous catalysts, and also contribute to understand the development of photocatalytic systems for more complex organic reactions.

Future Work:

1. The combination of Ag with other transition metal should be designed as new of supported alloy NP photocatalysts. As we know, besides Cu, there are many transition metals which are catalytically active and widely used in thermal catalytic reactions. They can provide active sites in photocatalytic reactions. Ag has strong absorption in visible light due to the LSRP effect and it is stable in air. Combining the two advantages, the more stable and active alloy NP photocatalysts could be developed for a wide range of organic syntheses.

2. The plasmonic nanostuctures is well-known of the tuneable LSPR wavelength with particle geometry such as size, shape and composition. This inspires us to design nanosturctures that can efficiently absorb visible light by manipulating the properties in catalyst preparation.

3. The main aim of our research is to utilise solar energy to enhance organic reaction rate, therefore the impact factor of reaction rate should be investigated in detail. The affinity of the catalysts to the reactant is a significant factor. For our research, we use supported metal NPs as photocatalyst, therefore to change the affinity of support to the reactant is another potential way to enhance reaction rate. Therefore the improvement of support could be an important direction to enhance the photocatalyzed reaction rate.